Republic of Iraq
Ministry of Higher Education
and Scientific Research
University of Kerbala
College of Science
Department of Chemistry

Synthesis and Characterization of Organosilicon Catalyst for Cellulose Hydrolysis

A Thesis

Submitted To the Collage of Science, Kerbala University In Partial Fulfillment of The Requirement for Master Degree In Chemistry

By

Hussein Salman Sobh Al- Tai

B. Sc. University of Kerbala (2013)

Supervision by

Assist. Prof. Dr. Hayder Hamied Al-Hmedawi

2017 A.C 1439 A.H

بِسۡمِ ٱللَّهِ ٱلرَّحۡمَٰنِ ٱلرَّحِيمِ

﴿يَرۡفَعِ ٱللَّهُ ٱلَّذِينَ ءَامَنُواْ مِنكُمۡ وَٱلَّذِينَ أُوتُواْ ٱلۡعِلۡمَ دَرَجَٰتٖۚ وَٱللَّهُ بِمَا تَعۡمَلُونَ خَبِيرٞ﴾

صدق الله العلي العظيم

سورة المجادلة اية11

Dedication

To those who sacrificed themselves for the sake of the homeland and the sanctities to the souls of the martyrs of the popular populist crowd and the heroic security forces

جمهوريه العراق

وزارة التعليم العالي والبحث العلمي

جامعة كربلاء

كلية العلوم

قسم الكيمياء

تحضير وتشخيص محفزات عضوية- سلكونية لغرض تحلل السليلوز

رسالة مقدمة الى كلية العلوم- جامعة كربلاء

كجزء من متطلبات نيل درجة الماجستيرفي الكيمياء

من قبل

حسين سلمان صبح الطائي

بكاليوريوس علوم في الكيمياء-جامعة كربلاء (2013)

باشراف

أ.م.د. حيدر حميد الحميداوي

2017 A.C 1439 A.H

الاهداء

الى الذين ضحوا بانفسهم من أجل الوطن والمقدسات

الى أرواح شهداء الحشد الشعبي المقدس والقوات الامنية البطلة.

الخلاصة

في هذه الدراسة تم تحضير سيليكات الصوديوم من رماد قشر الأرز (RHA)، ثم مفاعلتها مع 3 - (كلوروبروبيل) تراي ايثوكسي سايلين (CPTES) عن طريق تقنية بسيطة للمحلول-الجيلاتيني (sol-gel) لتحضيرRHACCl ثم تستبدل ذرة الكلور بذرة اليود لتحضيرامركبRHACI بعد ذالك الثيوريا تدعم مع RHACI لتكوين محفزجديد nanoheterogeneous RHATU-SO_4H. وقد استخدمت العديد من التقنيات لإثبات استبدال مجموعة الكلورو بمجوعة اليود وكذلك تكوين المحفز مثل الا شعة تحت الحمراء (FT-IR) وتحليل العناصر (CHNS) وتشتت الاشعة السينية (XRD)والمجهرالالكتروني الماسح (SEM) وتحليل التكسر الحراري (TGA/DTG) وتحليل امتزاز-وازالة الامتزار النتروجين(BET)و XPS والتي اثبتت صحة الصيغة التركيبية المتوقعة للناتج، حيث ان ظهور حزمة امتصاص اصرة C-I- في المنطقة المتوقعة $580\ cm^{-1}$ يؤكد تكوين المركب المتوقع، لانها غير موجودة في امتصاص (FT-IR) لمركب RHACCl وتحليل العناصر لم يظهر تغير في عدد ذرات الكاربون أيضا اما التحلل الحراري (TGA/DTG) يظهرمراحل تكسرللجزء العضوي ضمن هيكل المركب RHACI ومن تحليل امتزاز النتروجين، تم حساب المساحة السطحية والتي تساوي $410\ m^2/g$ كما أظهر تقنية (XPS) حزم امتصاص في618.5 ev تعزى الى اليود C-I وكذالك حزم ev (284, 531.0 , 101.5) تعزى لكل من الكربون والاوكسجين والسيلكون على التوالي، كل هذه التقنيات تعطي أدلة جيدة على صحة الصيغة التركيبية للمركب المحضر RHACI. في حين شخص المحفز RHATU-SO_4H من خلال ظهور حزة امتصاص ضمن المنطقة المتوقعة للامين NH- , C-N وO=S=O في تركيب المحفز مما يؤكد تكوين المركب المتوقع لانها غير موجودة في امتصاص (FT-IR) للمركب RHACI، واكدت نتائج تحليل العناصر زيادة في نسبة الكربون والهيدروجين وجود النيتروجين والكبريت التي لم تكن موجودة في تركيب RHACI كما يظهرتحليل التكسر الحراري (TGA/DTG) مراحل مختلفة من خسارة الوزن تعزى إلى فقدان كتلة من الجزء العضوي في هيكل المحفز ايضا أظهرت BET المساحة السطحية$357\ m^2/g$ للمحفز RHATUSO_4H وباستخدام هذا المحفز فأن نسبة تحلل السليلوزالى الكلوكوز 81% في 140°C لمدة 16 ساعة أخيرا فأن المحفز يتميز بسهولة تكوينه وثباته اثناء استخدامه في تحلل السليلوز,كما يمكن استخدامه عدة مرات بدون فقدان الفعاليه التحفيزية.

SUPERVISOR CERTIFICATION

I certify that this thesis was prepared by **Hussein Salman Sobh** under my supervisor at the Chemistry Department, College of Science, Karbala University, as a partial requirement for the degree of Master of Science in Chemistry.

Signature

Name: **Assist. Prof. Dr. Hayder Hamied Al-Hmedawi**

Address: **University of Kerbala**

Date:

HEAD OF DEPARTMENT CERTIFICATION

In view of the available recommendation by supervisor, I forward this thesis for debate by the examining committee.

Signature

Name: **Assist. Prof. Dr. Baker Abid Al-Zahra Joda**

Address: University of Kerbala

Date:

Report of Linguistic Evaluator

I certify that the Linguistic evaluation of this thesis was carried out by me and it is linguistically sound.

Signature

Name:

Address:

Date:

Report of Scientific Evaluator

I certify that the scientific evaluation of this thesis was carried out by me and it is accepted scientifically.

Signature

Name: **Asst. Prof. Dr. Basim Ibrhim Mehdi**

Address: **University of Baghdad**

Date:

Examination Committee Certification

We, the examining committee certify that we read this thesis "**Synthesis and Characterization of Organosilicon Catalyst for Cellulose Hydrolysis**" and have examined the student (**Hussein Salman Sobh**) in its contents and that our opinion, its adequate as a thesis for the degree of Master of Science in chemistry.

(Chairman)

Signature:

Name: Prof. Dr. Emeritus Falih H. Mousa

Address: University of Baghdad

Date:

Signature:

Name: Assis.Prof**.** Dr. Mohammed Hamid Said

Address: University of Babylon

Date:

Signatur:

Name: Assist. Prof**.** Dr. Haitham Dalol Hanon

Address: University of Kerbala

Date:

Signature:

Name: Assist. Prof. Dr. Hayder Hamied Al-Hmedawi

Address: Univrsity of Kerbala

Date:

Approved by the council of the college of science in its session No. in

/ /

Signature:

Dean of college of science, University of Kerbala

Name: Prof. Dr. Amir Abdul Ameer

Address: University of Kerbala

Date:

Acknowledgment

Praise is to God and thanks first, civilian strength and patience in all my life, the virtue of this work is complete.

My thanks to supervisor **Assist. Prof. Dr. Hayder Hamied Al-Hmedawi** for his support during the work of moral support and science provided to me.

I would also like to thank the head of Chemistry Department **Assist. Prof. Dr. Baker Abid Al-Zahra Joda** and all staff of the department of chemistry for helping me during the period of work as well as my thanks and gratitude are present to all the Deanship staff in the College of Science.

I also extend my heartfelt thanks to my mother, all my brothers and my dear wife for their support in everything.

Finally, to my loved friends, I extend my thanks and gratitude for their moral support and standing by my side in the hardest stages of research.

Thank you for all

Hussein Salman

Abstract

In this study the sodium silicate was prepared from rice husk ash (RHA), after that sodium silicate was transformed to functional silica with 3-(chloropropyl)triethoxysilane (CPTES) via simple sol-gel technique to prepared RHACCl. Then a chloro atom in RHACCl replaced in an iodo atom to form new compound RHACI. Thiourea immobilized with RHACI to synthesis new nanoheterogeneous catalyst labeled as RHATU-SO_4H. Many techniques have been used to characterization the synthesis of RHACI such as FT-IR, CHNS, XRD, SEM, TGA/DTG, BET and XPS. The FT-IR clearly indicated absorption band at 580cm^{-1} attributed to stretching vibration of C-I bond also the elemental analysis shows same percent in carbon atom of RHACCl. The thermal analysis (TGA/DTG) has different stages of loss mass attributed to loss mass of organic part and silanol in the RHACI. BET indicated the surface area for RHACI was 410 m^2 g^{-1} . XPS showed bending energy band of I 3d at 618.5ev assigned to C-I bond and C 1s at 284 ev, O 1s at 531.0 ev and Si 2p at 101.5 ev. All these techniques give good evidence for successful synthesis of RHACI. Nanohetrogeneous catalyst RHATU-SO_4H characterized by FT-IR, CHNS, XRD, SEM, TGA/DTG and BET. The FT-IR clearly indicated the presence –NH, O=S=O and C-N absorption band of catalyst absorbed .The elemental analysis result showed an increase in carbon percentage and the presence of nitrogen and sulfur which are not found in RHACI. The thermal gravimetric analysis (TGA/DTG) appears different stages of loss mass attributed to loss mass of the organic moiety in the catalyst structure. BET showed the surface area for RHATU-SO_4H was 357 m^2 /g, the hydrolysis of cellulose gives glucose yield 81%at 180 ℃ for 16 h. The catalyst was simple synthesis, more stable during hydrolysis of cellulose in addition to reusability without less catalyst activity.

TABLE OF CONTENTES	
Subject	**Page**

Chapter one-introduction

LIST OF TABLES

LIST OF FIGURES

LIST OF SCHEMES

LIST OF SYMPLES AND ABBREVIATIONS

AC-SO_3H	Active carbon sulfate
BET	Burnuar-Emmett-teller
BJT	Berret-Joyner-Halenda
BE	Binding energy
Cond.	Condensation
CPTES	3-Chloropropyltriethoxysilane
CPTMS	3-Chloropropyltrimethoxysilane
CP-SO_3H	Chloromethyl polystyrene
Ca.	Calculated
DMF	Dimethylformamide
DMSO	Dimethylsulfoxide
DNS	Dinitrosalicilic acid
DTG	Deferential thermal Gravimetric
Et_3N	Triethylamine
Fig.	Figure
H2	Hysteresis loop type 2
MOF	Metal-organic framework
$PrSO_3H$-SiO_2	Pronsted acid silica
p/p°	Relative pressure
RHACCl	RHA immobilized with 3- (chloropropyl)triethoxysilane
RHACI	RHACCl replacement with NaI

RHATU-SO_4H	RHA Immobilized with thiourea (heterogeneous catalyst)
RHA-Ga	RHA immobilized with Gallium
RHA-Fe	RHA immobilized with iron
RHA-In	RHA immobilized with indium
SPS-DVB	Sulfonated poly (Styrene-co-drivinyl benzene)
SUCR-SO_3H	Sucralose-derived solid acid
TEOS	Tetraethylorthosilica
TU	Thiourea

CHAPTER ONE

Introduction

1.1General entrance

The rate of chemical reaction increases by catalysis process due to the partnership of substance called a catalyst. To become catalyst have important area of chemical research since metals started used to be metal in 1969s by von Marum for dehydrogenation of alcohols. The term "catalyst" was introduced as early as 1836 by John Jacob Berzelius when he supposed that catalyst had abilities that called cause the convergence of chemical substance. Most catalysts are liquid or solid, but they may also be gases. The reaction of catalyst is a cyclic process. According to a simplified model the reactants or reactant form complex with catalyst by opening pathway for their transformation in to the product or products [1]. There are two types of catalyst heterogeneous and homogeneous.

1.1.1 Heterogeneous and homogeneous catalyst

Homogeneous catalysis is catalysis in a solution by a soluble catalyst. Strictly speaking, homogeneous catalyst refers to catalytic reactions where the catalyst is in the same phase as the reactants. Homogeneous catalysis applies to reactions in the gas phase and even in liquid phase. Heterogeneous catalysis is the alternative to homogeneous catalysis, where the catalysis occurs in the different phases as during of reaction such as solid-liquid, solid-gas and liquid-gas.

The main majority of practical heterogeneous catalysts are solids and the main majority of reactants are gases or liquids. Heterogeneous catalysis is paramount importance in many areas of the chemical and energy industries.

Heterogeneous catalysis has attracted Nobel prizes for Fritz Haber and Carl Bosch in 1918, Irving Langmuir in 1932, and Gerhard Ertl in 2007.

The reaction of heterogeneous consists reactant adsorption form liquid phase onto surface of solid, surface reaction of absorbed types and desorption of product into the liquid [2],then make weak bond onto solid surface during occurrence chemisorption. The heterogeneous catalyst has number of advantage over homogeneous catalyst as simplicity in synthesis process, prevention of the production of salt wastes or reagent and reusability of solid catalyst [3]. Scheme1-1Shows the mechanism of heterogeneous catalyst include diffusion of reactant onto solid surface, chemisorption on the surface of solid, desorption of reactant from surface and diffusion reactant to product.

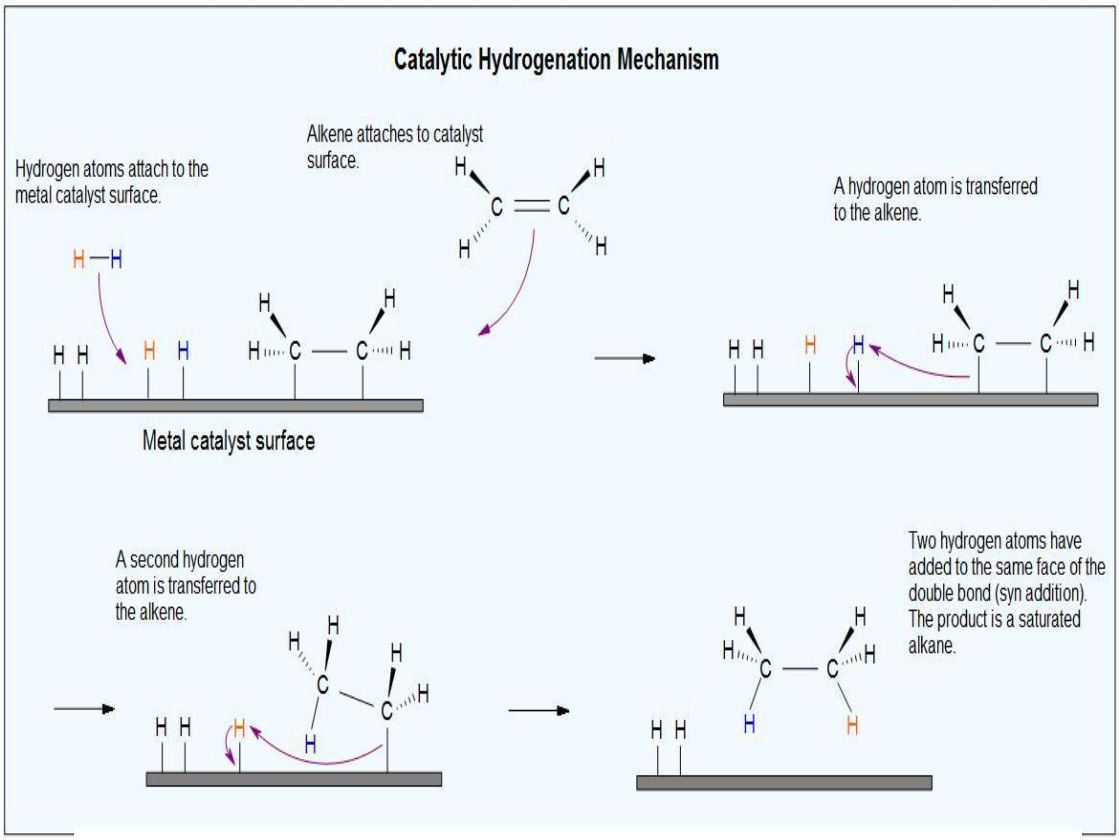

Scheme 1-1: Mechanism of heterogeneous catalyst

Rice husk ash (RHA) was used as heterogeneous catalysts to synthesize a large of catalysts such as RHA-Ga, RHA-In and RHA-Fe catalysts by direct incorporation of the respective ions into rice husk ash silica at room temperature. The prepared catalysts were used to catalyze the benzylation of p-xylene (p-Xyl) with benzyl chloride (BC) [4].

1.2 Rice and rice husk

Rice cultivation is the principal activity and source of income for million of household around the globe, and the several countries of Asia and Africa are highly depended on rice as a source of foreign exchange earnings and government revenue [5]. The rice covers 1% of surface area of the earth and it is one of the first food sources for billions of people world rice production was 481.54 million metric tons in 2016-2017 [6]. This sustainable biomass fuel consists of approximately 40%wt cellulose, 30%wt lignin and 20%wt silica [7]. Rice husks (RH) are a by-product of rice milling industry. These husks cause serious disposal and pollution problems of environmental. However, due to the presence of a high content of silica in this husk, it was thought advantageous to use the silica as support for much reaction [8]. The function of husk is protecting rice grain during the growing season. Rice husk shown in Fig.1-1.

Fig.1-1: Rice grains covered in husk in phase spike

1.2.1 Rice husk ash

The rice husk ash (RHA) is obtained by burning of rice husk at temperature between 500 °C to 800 °C in fume furnace. It has rich content of non-crystalline silica form (amorphous silica) and the high than crystallization accrued [9]. Rice hull produces ash which has a high silica content of about 90-95% after complete combustion. In addition, rice ash produces two colored ash after a period pruning, the white-grey attained at complete combustion [10]. This silica in the ash undergoes structural transformation depends on the condition (temperature and time) during burn [11]. The ash then employed as the starting material for extraction of silica [12]. Burning the husk in space causes environmental pollution as Fig.1-2.

Fig. 1-2: Rice husk burned as a waste and causes environment pollution pollution

1.2.2 Components of rice husk ash

The composition chemical of rice husk is different from sample to another. The differences are in climatic, geographical condition, type of paddy etc. [13]. The chemical analysis of rice hull was shown in Table 1-1. Inorganic component which around 20% of dry rice husk from this silica represents about 94% wt and 6wt% Fe_2O_3, Al_2O_3, CaO, MgO, MnO and SiO_2 [14]. Major organic component in the dry rice hull is shown in Table 1.2 50% hemi-cellulose and cellulose, 26% lignin and 4% other organic compound like protein, oil [15].

Table 1-1: Chemical analysis of the raw RH [14]

constituent	**Content (Wt %)**
Organic material and moisture	73.87
Al_2O_3	1.23
CaO	1.24
MgO	0.21
MnO	0.074
Fe_2O_3	1.28
SiO_2	22.12

Table 1.2: Organic constituents of RH [15]

constituent	**Amount present in RH (wt %)**
α- Cellulose	43.30
Lignin	22.0
D-xylose	17.52
L-arabinose	6.53
Methylglucuronic acid	3.27
D-galactose	2.35

1.3 Sol-gel technique

The sol-gel process, as its name indicates includes the manufacture of inorganic materials by the creation of colloidal suspension (sol) and gelation of the sol to form a wet gel (globally linked solid matrix), which later during formation "dry gel" state (xerogel) [16]. The sol-gel is synthesis route inorganic non-metalic material. Monomer reaction, oligomers or colloids can be utilized as initial material that has to be "activation" in order to undergo a poly condensation step and to form polymeric network [17]. All sol-gel methods can be classified as alcohol-based or aqueous as called, aqueous-based system which is carried out in the presence of water, while alcohol-based system generally excludes build-up of water until the hydrolysis stage also can be classified according to non-alkoxide or alkoxides [18]. The formation of sol solution consists of the employ of solvent. These solvents are usually organic alcohols. The first objective of the solvent is soluble solid starting material that is also employed to dilute liquid precursor and minimize the influence of the concentration gradients. The particular solvent employed can affect parameter, such as temperature of crystalline, pH of solution, and the particle morphology [19]. The method involves condensation and hydrolysis metal alkoxides [$Si(OR)_2$] like tetraethylorthosilica [TEOS, $Si(OC_2H_5)_4$] or inorganic salt such as sodium silicate (Na_2SiO_3) in the presence of the base or mineral acid[20]. Fig.1-3 shows the typical of sol-gel process.

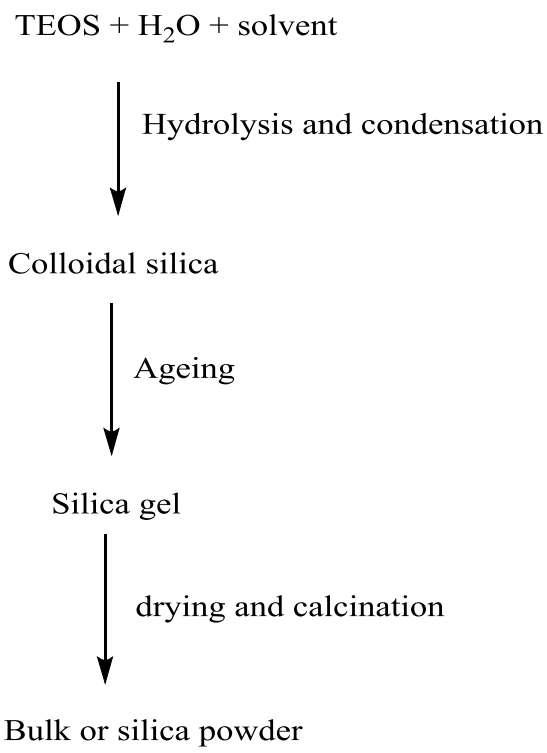

Fig.1-3: Flow chart of a typical sol-gel process

TEOS have general reaction that leads to the preparation of silica particle in the sol- gel technique. It can be shown in scheme 1-2 [21].

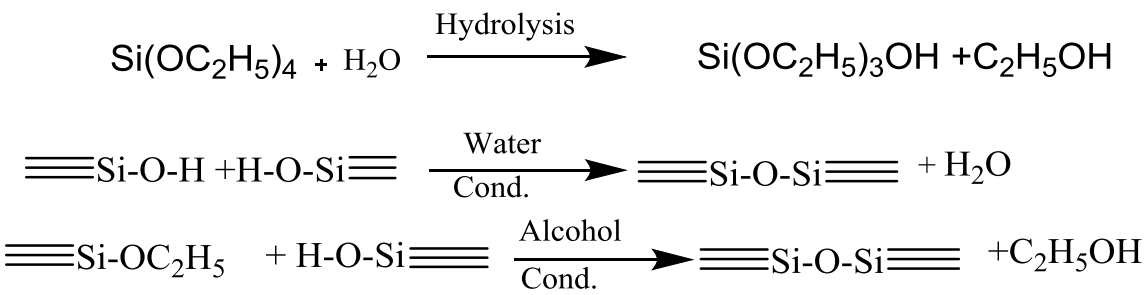

Scheme 1-2: Formation of silica particle.

The decomposition of TEOS particle forms silanol groupes. The condensation/polymerization among the group of silanol and among ethoxy groups and silanol groups forms siloxane bridges (≡Si-O-Si≡) that for entire structure of silica. The synthesis of silica particles can be classified into two

stages, growth and nucleation. Two models, monomer addition and controlled aggregation have been proposed to describe the growth nucleation of silica [22-23]. It is shown in Fig 1-4.

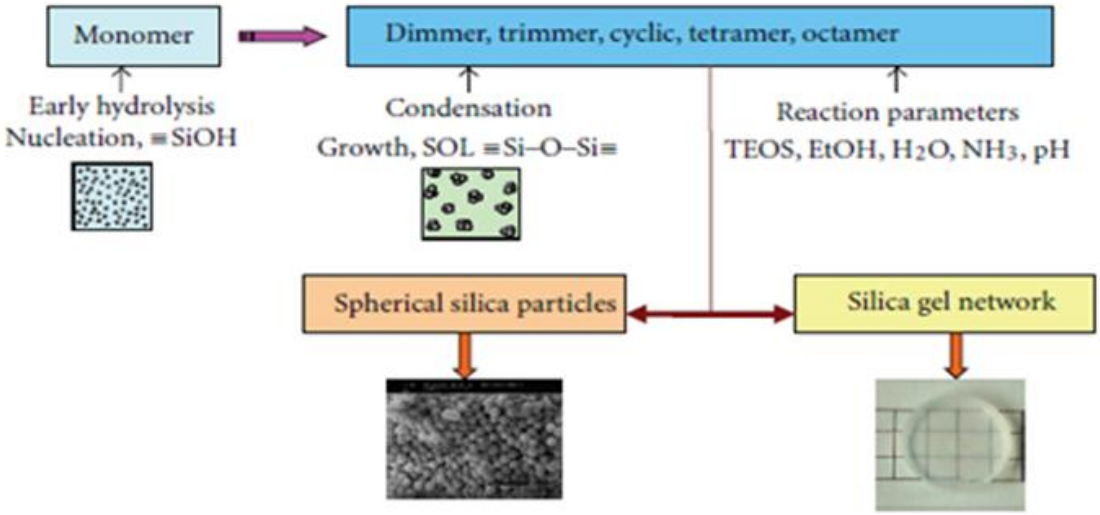

Fig. 1-4: Formation of silica by sol-gel process

1.4 Crystalline and Amorphous silica

Silicon dioxide, also known as silica (from the latin silex) is silica oxide with formula SiO_2 or $SiO_2.XH_2O$ [24]. In nature, silica is inert and it is founded in crystalline and amorphous shape. The crystalline form the main portion of soil sand and different form such as mineral likes quartz, cristobalite and tridymite [25]. Amorphous silica is a dispersed form which is greater highly hydrated compared with crystalline form and exists as infusible earth [26]. The scheme 1-3 shows the structure tetrahedral of silica in nature.

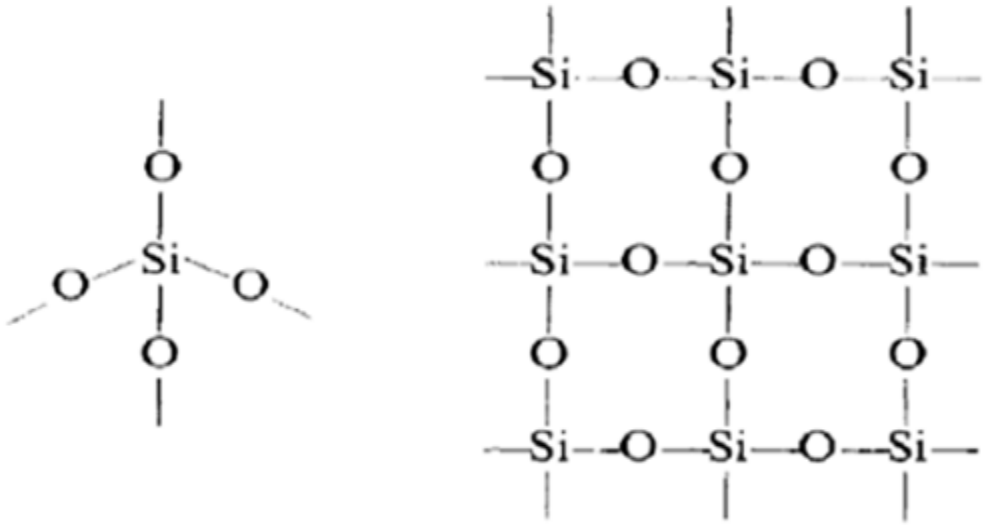

Scheme 1.3: Structure of silica showed bonded of silicon with four oxygen atoms to form tetrahedral shape [24].

Silica founded in numeral amorphous named dispersed system as described in Table 1-3.

Table 1-3: Amorphous dispersed silica

Technique	Procedure	Ref.
Silica sol (colloidal):	It is an important type of amorphous silica that can be synthesis by sol-gel. Poly condensation and polymerization of dissolve silicate by adjusting the pH using base or acid.	[27]
Silica hydrogel	It is solid, coherent and containing three dimensional networks, which can be synthesis by proceeding of condensing reaction until the point of gelation.	[28]

Silica xerogel	It is partial distorted gel, which can be formed through the dehydration process of hydrogel and disappearance its pore filling liquid (often water).	[29]
Silica aerogel	It is a porous ultra light material with volume of high pore that can be synthesis during the process of supercritical drying of gel and replacing the liquid component with gas.	[30]
Precipitated silica	It is dry silica with small distance characteristics structure. It happen when the silica particles are coagulated as loose aggregation in the aqueous medium.	[31]

Contrast among amorphous and crystalline silica shapes creates from the linked of the tetrahedral units. Amorphous silica contains of non-recurring network of tetrahedral where each oxygen corner linked to adjacent tetra-hydra. Although there are no long range periodicals in the network their remains significant ordering at length scales well beyond the SiO bond length [32]. The amorphous silica structure is very "open".

1.5 Nature surface of amorphous silica

Studies on the silica began in 1930s and ran to the understanding the nature of the silica surface [33]. Due to the considerably spectral and the chemical data, it has become clearly that silica has two variety active groups i.e. the siloxane (=Si-O-Si) in the bulk and number form of silanol group (=Si-OH) on the silica surface. Depending on the NMR studies, there are

found three types of siloxane groups (≡Si-O-Si≡) which can be expressed by following expression Q = $Si(OSi)_n (OH)_{4-n}$ where n=2-4 which states to the numeral bridging bond (O-Si) bonded to the central Si atom, i.e. Q^2, two siloxane linked to the centeral Si atom. Q^3, each central silicon atom bonded to three siloane. Q^4, each central silicon atom linked with four siloxane bonds. Fig.1.5 show in moreover experimentally there are three types of silanol group on the silica surface: isolate silanol group (each silicon atom linked with single hydroxyl) vicinal called when the silanol group bonded by intermolecular hydrogen bond with other silanol group, while the geminal silanol called when the two hydroxyl bonded on the same silicon atom $\equiv Si(OH)_2$ [34]. The silica surface can be activated using modification reaction with organic nucleophile to obtain new bond, i.e ≡Si-O-C=, ≡Si-O-C≡ by way reaction of the functional group of silanol [35].

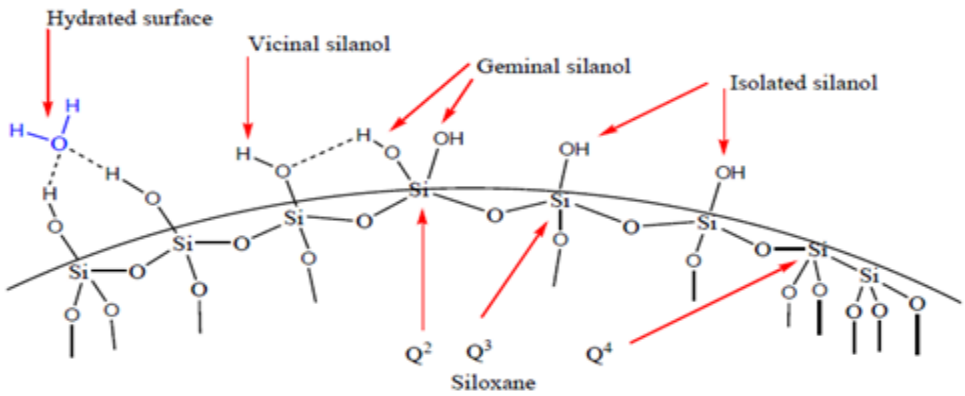

Fig 1-5: Various type of silanols and siloxanes group on the matrix of silica.

The silica surface tends to have tetrahedral configuration and their free valance in aqueous medium becomes saturated through hydroxyl group. The properties of a pure silica, as an oxide adsorbent, are determined in the first place by (i) The chemical activity of the surface that depended on the distribution and concentration of different type of hydroxyl (-OH) groups and on the presence of siloaxne bridges, (ii) the porous structure of silica [36].

1.6 Modification of silica surface

The studies reported that the major modification via approach occurred by the substance of reaction molecules through the silonal groups on the surface of silica [37]. The silica modified substance have many applications in catalysis [38].The modified procedure sung pure active silica gel can be useful at relative high temperature, being applied for hours at more than 373K. However, the conventional modifications of methods reach some desired [39]. There are two common approaches to create anchors to the surface of silica using the silanols to create siloxane bonds (Si-O-Si) or creating Si-C bond directly with surface silicon atom. The most common oragnosilanes used in wall modification are trifunctional modifiers such as $RSiX_3$ trimethtoxy or triethoxy silanes. The organic functional, R, is the strongly bonded to the surface through the siloxane bonds. The limited of the Si-O-Si-C linkage has received much attention, such siloxane bonds are bonded only stable in the pH range from 3-7.5 [40]. The immobilization of the silylating agents carried out two methods. The first method is to react the ligand complex through silalting agents, and then to immobilize the resulting ligand with the pre-formed silica in a heterogeneous reaction. The second method is to treat the post- polysiloxane with the complex group [28]. The two methods are shown in scheme 1-4.

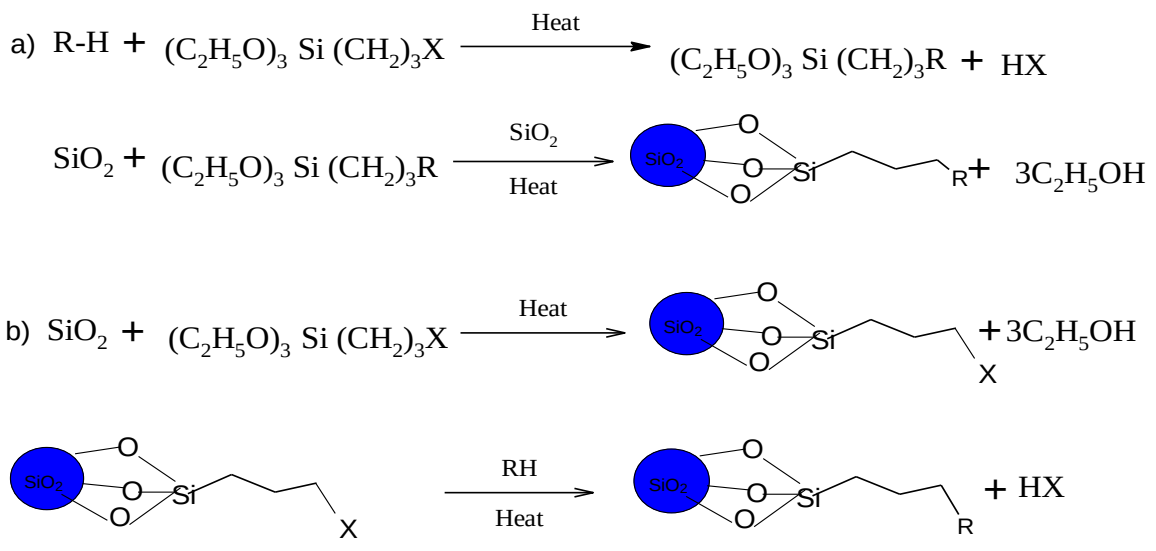

Scheme 1-4: (a) Reaction of the silylating agent with the ligand complex followed by immobilizes the resulting ligand onto silica. (b) Immobilizing of silylating agent onto silica followed by immobilizing the ligand complex.

1.7 Immobilization chloride systems on the silica surface

Silica modified with organic chloride functionalization of amorphous silica is important starting point for preparation of a wide variety of silica based material. The functionalization of organo-chloro silica which contains a C-Cl end group can be used for immobilizing other organic parts onto the silica surface. It can also be used as the starting material for the preparation of heterogeneous catalyst [41, 42], Chiral heterogeneous catalyst [43], Solids for hydrogen adsorption [44], after for the synthesis of florescence chemo sensor [45]. The surface functionalization of silica with 3-chloropropyltriethoxysilane (CPTES) was usually carried out by post synthesis methodize. In solid liquid mixed phase reaction [46]. The reaction needs to the refluxing in the toluene for 12h. The silica can also be functionalized to synthesis chemosenser by refluxing in toluene for 24h. This was trap by soxhlet extraction [47] with the various natural solvent.

After different specialists had details the functionalization of silica (which was per-dried at 100°C for 6h). By reflux it with CPTES in toluene [48], for18h. Demonstrated that's 3-(chloropropyl)triethoxysilane (CPTES) can likewise be utilized to functionalize response should be refluxed 96h at 160°C . A similar response was done by Sanderson et al [49], by the refluxing CPTMS with silica for 24h.Treated by soxhlet, Extraction with dichloromethane (DCM) for 12h. The concise audit above demonstrates that the present strategy to functionalization silica with CPTES requires high temperature, danger natural solvents and longer refluxing time. Recently study includes a novel strategy to functionalize silica with CPTES which is straight forward. That does not require dangerous reagent and inside does not sensible time of 6h without resorting to high refluxing temperature. This technique includes a one –pot analgamatitation of silica –CPTES complex sodium silicate acquired from RHA. The strategy brings about high yield of the surface adjusted silica from a shoddy waste result of the rice milling industry [50]. Scheme 1-5, Shows synthesis RHACCl from modification sodium silicate.

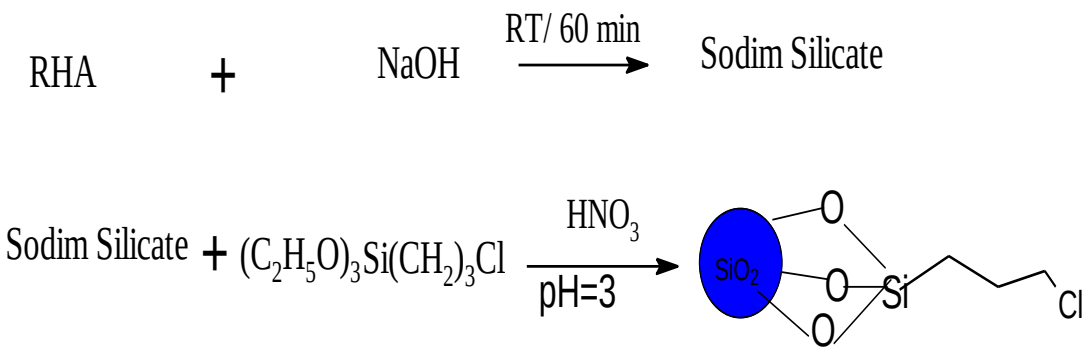

Scheme 1-5: Modification of silica with CPTES

1.7.1 Immobilization of organic molecule onto RHACCl

Table 1-4, Shows immobilization of some organic molecules onto RHACCl. The prepared heterogeneous catalysts showed different applications, some of them were used as esterification reaction, cyclization reaction, hydrolysis of cellulose, alkylation reaction and etc.

Table 1-4 Shows immobilization of some organic molecules onto RHACCl and applications.

Precursor	Organic molecule	Structure	Application	Ref.
RHACCl	Melamine	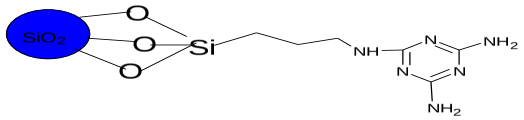	Esterification reaction.	[51]
	Dithiooxamide	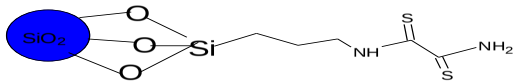	Esterification reaction.	[24]
	p-phenlyenediamine	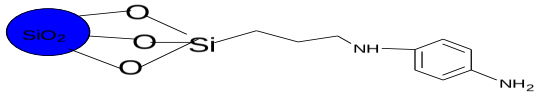		
	Schiff base	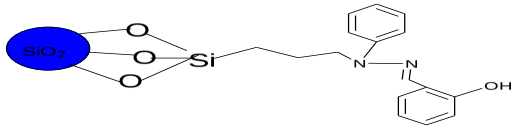	Hydrolysis of cellulose	[13]
		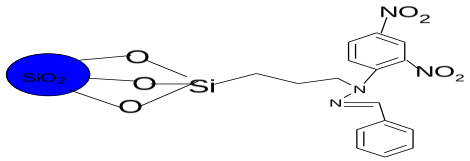		
	Urea	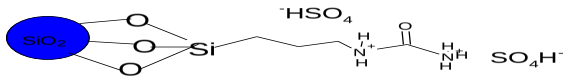	Cellulose hydrolysis	[52]
	Sulfaniline acid	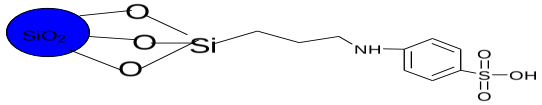	Alkylation reaction	[8]

RHACCl	Imidazole	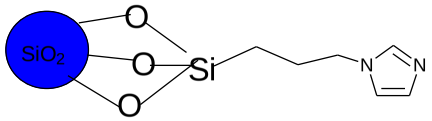	Catalyst reaction	[53]
	1-butylimidazole	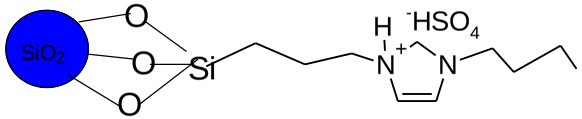	Cyclization reaction	[54]
	saccharine	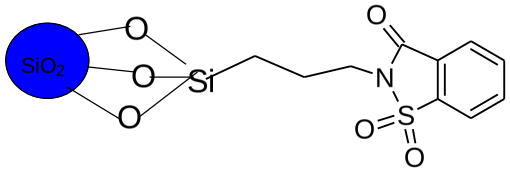	Esterification reaction	[55]
	L-phenylalanine-Ru(III) complex	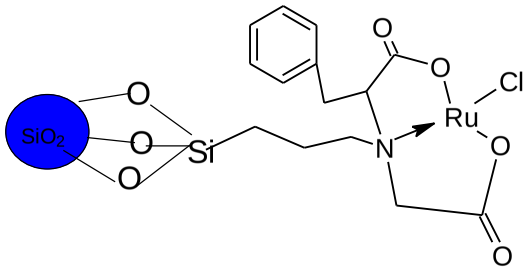	Esterification reaction	[56]

1.8 Thiourea

Thiourea is an organicsulfur compound with the formula $SC(NH_2)_2$. It is structurally similar to urea except that the oxygen atom is replaced by the sulfur atom but properties of urea and thiourea differ significantly. Thiourea is a reagent in organic synthesis thiouear refer to broad class of compounds with the general structure $(R'R''N)_2CS$ [57]. Urea/thiourea have hydrogen bonding tendencies to given donor group H-bonding donating urea/thiourea in someway related hydrogen bonding has been defined as proton transfer from donor group acid to the accepter group. The thiourea is a much acid than urea pKa=21.1 and pKa= 25.9 respectively in DMSO this is excepted that thiourea is consisting receptor establish stronger hydrogen bonding interaction and form more stable [58].

Thiourea used as catalyst, first homogenous thiourea catalyst are difficult to recycle and another issue is that thiourea catalyst known to deactivate through self-quenching, which is a self-assembly behavior due to catalyst-catalyst interaction such as dimerization or oligmerzation. Immobilization of thiourea functionality would be ideal to prevent both recycling and self-quenching issues at the same time; solvation issues of thiourea catalyst can also be suppressed. To immobilize the thiourea functionality various supports such as mesoporous silica, polymer and MOF have recently been reported [59]. Scheme 1-6, shows homogeneous thioura catalyst and heterogeneous catalyst

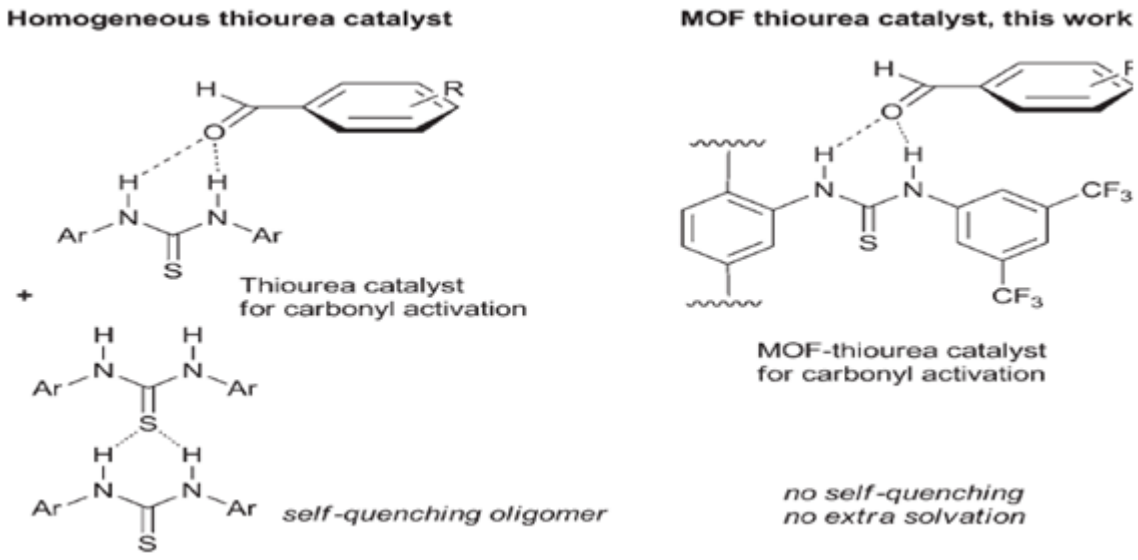

Scheme 1-6: Thiourea catalyst and MOF-thiourea catalyst

Thiourea based catalyst for sterker, mnnich, pictet-spengler and hydrophosphonylation reaction. These catalysts were proposed to activate a variety of carbonyl and sulfuoxide substrates for steroselsctive C-C bond forming reaction [60]. Scheme 1-7, thiourea- amine catalysts structure

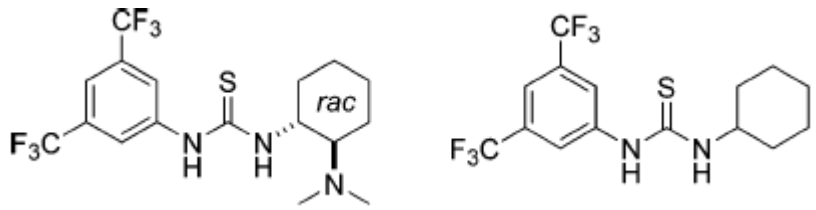

Scheme 1-7: Thiourea-amin catalyst structure

Aryl pyrrolidino amido-thioureas derived from α-amino acids have been prepared and used as catalysts in a number of asymmetric transformations scheme 1-8, they exist as mixtures of slowly interconverting amide rotamers. The compromising role of amide bond isomerism is analyzed experimentally and computationally. A modified catalyst structure that exists almost exclusively as a single amide rotamer is introduced. This modification is

shown to result in improved reactivity and enantioselectivity by minimizing .competing reaction pathways [61]

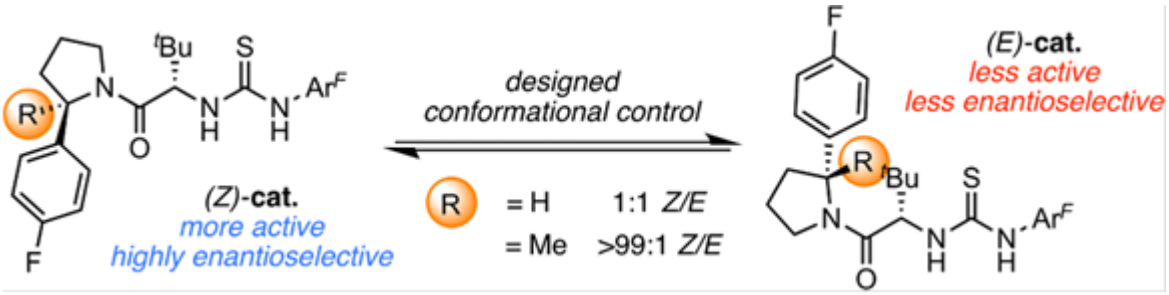

Scheme1-8: Prepared and used as a catalyst in a number of asymmetric transformation.

1.9 Cellulose

The cellulose has a number of applications such as engineering, scaffold, pharmaceutical, filiter media, nanosensor, adhesives. Skin mask, wound dressing, functional clothes papermaking [62]. Scheme1-9 shows structure of cellulose. The polysaccharide considers the main source of cellulose as the main constituent of the wall of cell of the plant, having agreement its name for this reason other cellulose consists material include, agriculture residue, water plant grasses, straws and other plant substance [63]. The nature source of cellulose based wood, hemp, cotton and linen [64]. Cellulose is a polymer has glucose unit's repeated molecular formula $(C_6H_{10}O_5)_n$ [65].

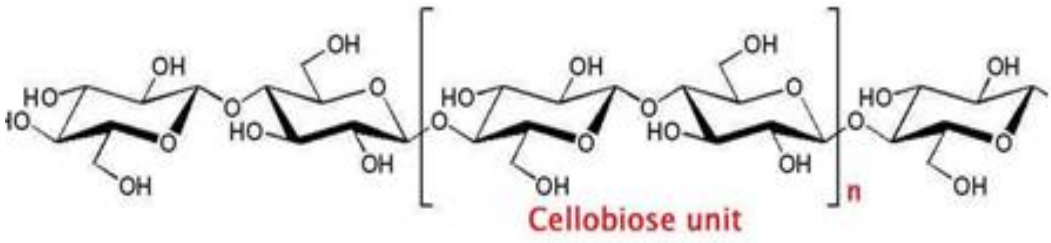

Scheme 1-9: Structure of cellulose.

1.9.1 Structure of cellulose

Cellulose is polymer of several D-glucose monomer units to form longer linear chain of cellulose. This D-glucose connected with each other by β-1,4-glycosidic bond to form linear chains of cellulose [66]. The fact that cellulose has more possibilities to have hydrogen bonds, both intermolecular- and intra with second chains or surrounding render it possible to organize in several ways [67]. This intermolecular and intra hydrogen bonds show in Scheme 1-10.

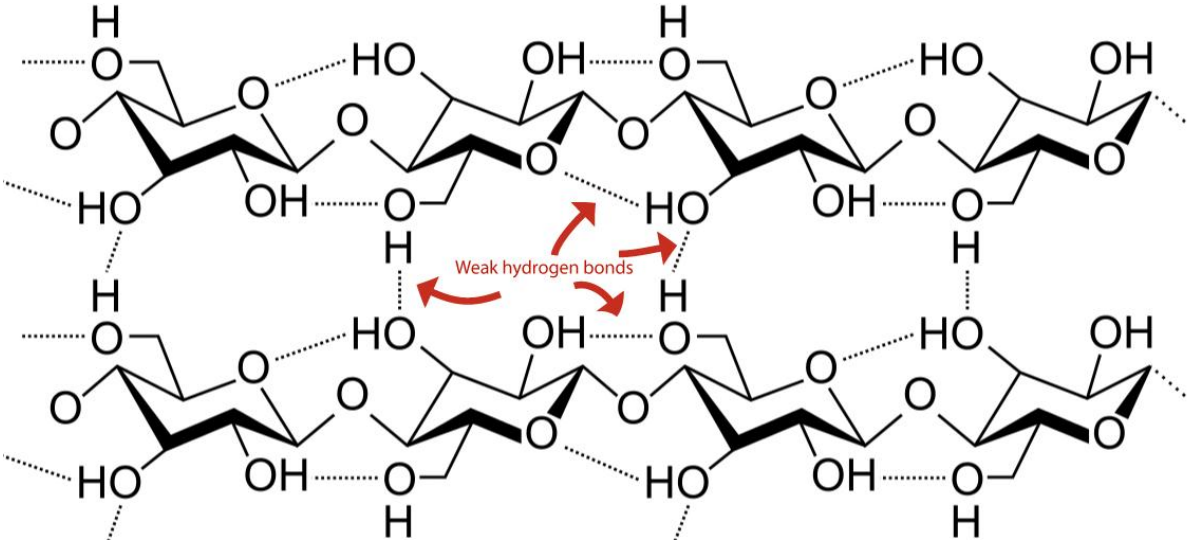

Scheme 1-10: Hydrogen bonding intermolecular and intra of cellulose structure

Cellulose has two groups, first group C_4-OH is called the non-reducing group or ends the second group original C_1-OH is called the reducing group. In addition carbonyl and carboxyl groups through chemical treatment such as bleaching chemical can be introducing to cellulose [68].

1.9.2 Hydrolysis of cellulose

Hydrolysis of cellulose carried out with diluted or concentrated acid, enzyme and other type of catalyst. Cellulose hydrolysis is the key technology for activity use of lignocelluloses because glucose can be efficiently

concentrated to different chemical biofuels, food and medicines [69]. Hydrolysis of cellulose as the entry point of biorefinery schemes in the important process for chemical and biochemical industries based on sugar, especially for fuel ethanol production however, cellulose not only provides renewable carbon source, but also offers challenge to researchers due to the structure recalcitrance. Considerable efforts have been devoted to the study of the hydrolysis of cellulose by enzymes, acid and supercritical water [70]. Changazh and zangabao etc [71], have been studied acid catalyzed hydrolysis through breaking hydrogen bonding and β-1, 4 glycosidic bond ionic liquid have been employed to form homogenous solution hydrolysis of cellulose prior to hydrolysis the Scheme 1-11, shown hydrolysis of cellulose by solid acid.

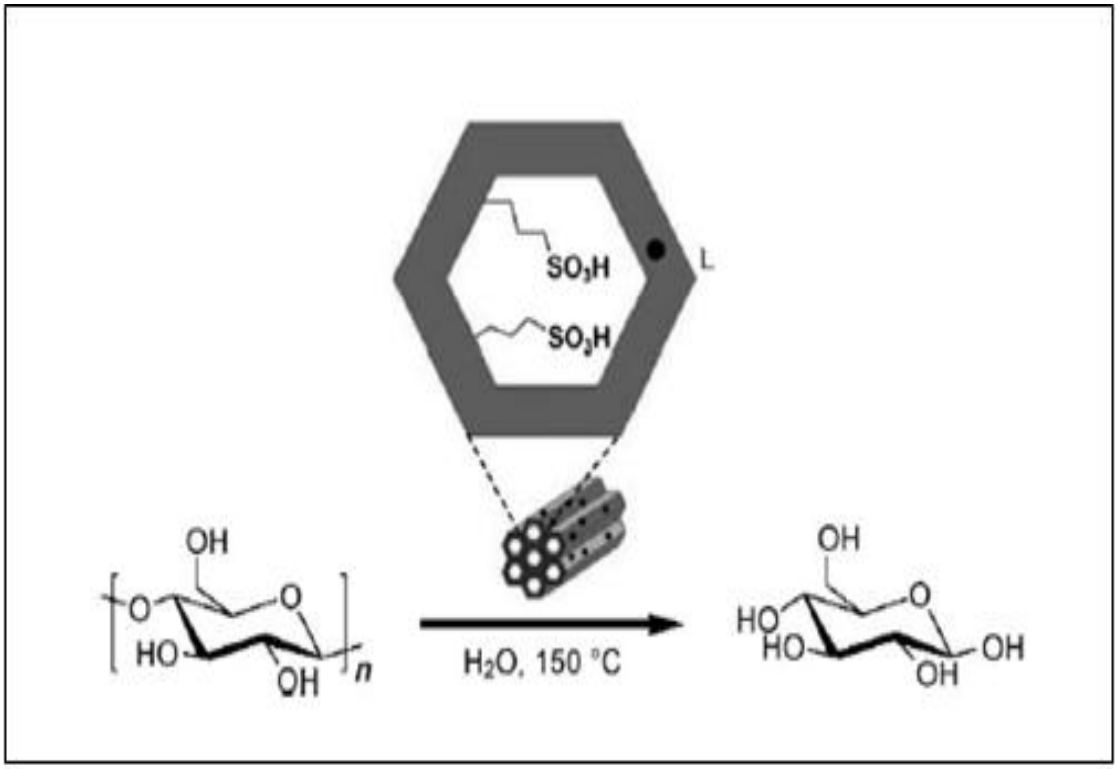

Scheme 1.11: Solid acid- catalyst hydrolysis of cellulose to form glucose.

Acid hydrolysis is most commonly used method for degradation of cellulose to glucose through hydrogen ions (H^+) penetrated cellulose molecules prompting cleavage of glycosidic bond (β-1,4). This hydrolysis depended on the cellulose source and especially, the hydrolysis reaction condition (i.e. the type and concentration of acid, time of reaction and reaction temperature [72]. Sulfuric acid hydrolysis of native cellulose fibers causes breakdown of the fiber in to rodlike fragment. These highly crystiline cellulose needles form stable aqueous suspension due to solfate groups, which have been introduced during the hydrolysis through esterification of surface hydroxyl groups [73]. There are several of methods for hydrolysis of cellulose in Table 1-5.

Table 1.5. Hydrolysis of cellulose to glucose by different catalyst.

Catalyst	Method	Time °C	Temp. °C	Solvent	Glucose yield%	Ref.
Ru/AC-SO3H	Acid hydrolysis	5h	245	Water	50	[74]
AC-SO3H	Acid hydrolysis	3 h	100	Water	64	[75]
$PrSO_3H$-SiO_2	Acid hydrolysis	4 h	110	Water	63	[76]
H_2SO_4	Acid hydrolysis	12	285	H_2O	90.8	[77]
Fe-GO-SO3H	Acid hydrolysis	9 h	75	Water	50	[78]
Silica with Zr,$TiO_2Al_2O_3$	Novel silica catalyst thermal condition and ball milling	12h	160	Water	50	[79]
Fe_2O_4-SBA-SO3H	Acid hydrolysis	2 h	130	Water	50	[80]
P-toluene sulfuric acid	Acid hydrolysis	3h	160	Water	30.3	[81]
CP-SO3H	Acid hydrolysis	10h	110	Water	93	[82]
Tungsted aluminum	Acid hydrolysis	24h	190	Water	42	[83]
H_3PO_4	Acid hydrolysis	6h	190	Water	65	[84]
SPS-DVP-SO_3H	acid hydrolysis	8h	190	Ionic liquid	48	[85]
CoFe-SiO_2-SO_3H	Solid acid	3h	150	Water	7	[86]
SUCR-SO_3H	Solid acid	24	120	Water	55	[87]

1.10 The equipment's used in this study

1.10.1 Nitrogen adsorption analysis

N_2 adsorption-desorption measurement has been used to determine the physical textural properties including surface area pore size distribution and pore volume per gram. This technique is based on the physical adsorption of gas (general N_2) on the internal and external surface of solid [88]. N_2 sorption analysis works under a constant temperature (usually 77k), by measuring the amount of gas adsorbed at each relative pressure compared to the (atmospheric pressure). The adsorption-desorption isotherm can be thus obtained. The isotherm of the mesopours materials studied here is of types IV according to IUPAC classification. Adsorption wonder initially examined and clarified by Langmuir (1930) [89]. Barrett, Joyner-Halenda (BJH) approach is widly used for calculation of the pore size. The pore volume is calculated from the maximal amount of absorbed liquid nitrogen around p/p=0.98. The calculation of the surface area is based on the BET (Berrunt, Emmett and teller) [90]. This theory which analysis developed in 1938 based on Langmuir adsorption model [91]. Fig. 1-6, shows instrumental of N_2 adsorption-desorption

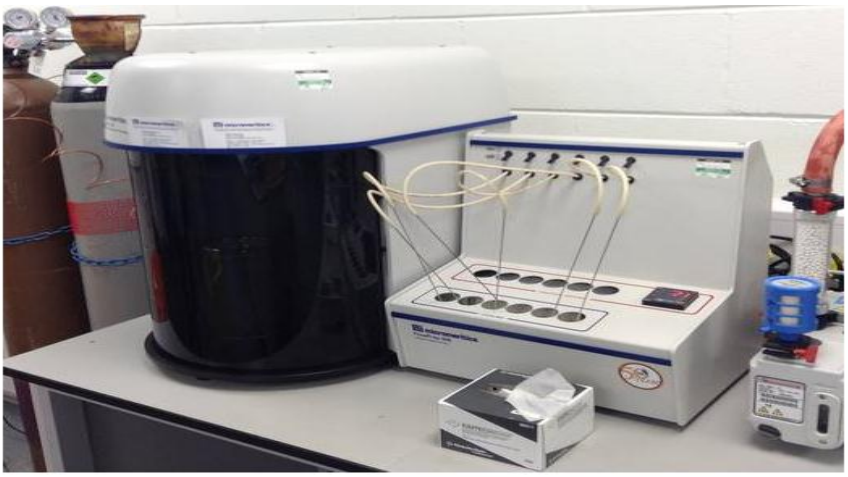

Fig. 1-6: N_2 adsorption-desorption instrument.

1.10.2 X-ray powder diffraction (XRD)

X-ray diffraction (XRD) is the one of most important catrcterization tools used in solid state chemistry and material science [92]. X-ray impedance is inferred the convocation between x-ray and matter must be considered. There are three approached sorts of cooperation in the important vitality run. In the principle, electron might be freed from their bound nuclear states during the time spent photoioaztion since vitality and force are exchanged from the approaching radiation to the energized electron, photoionzation fall in to the dispersive forms. Likewise, there exists a moment sort of inelastic dispersing that the poaching X-ray pillar may experience, which is called Compton dispersing. Likewise in this procedure vitality exchanges to an electron which prose EDX examination, nonthelss, without discharging the electron from the particle. At long last, X-ray might be scattered flexibly by electrons, which is called Thomson dispersing. In this last procedure the electrons wave like aHerz dipole at recurrence of the approaching bar and turns into a

wellsprings of dipole radiation [93]. The wavelength λ of X-ray is preserved for transom dispersing forms said above. It is the Thomson part in the dispersing of X-ray that is made utilization of in basic examination by X-ray distraction [94]. XRD method can derive the way of examined test, regardless of whether shapeless or crystalline structure and in addition basic date can along these line be found from the leering of dissipating force and plot for instance, approximated as rehashing separation in the permeable materials, the aggregate of a pore breath and a pore divider thankless can be assessed base on the separating computed from the Bragg condition [95]

$$n\lambda=2d\sin\theta$$

Where n is a whole number, λ is the wavelength, d is the detachment between planes and θ is the diffraction point. Fig.1-7, showed the instrument of XRD.

Fig. 1-7: X-ray diffraction (XRD) instrument.

1.10.3 Scanning electron microscope (SEM)

SEM is standout amongst vigorously utilized instrument in the scholastic lab, research in quire about area and industry. The electrons interaction with the particle that make up the sample producing singles that contain information about the specimen surface topography composition and different properties, for example, electrical conductivity. Amid SEM inspection abeam is cantered around a post volume of the example brining about the exchange of the vitality to the spot. These besieging electrons, too eluded as primary electrons, remove electron from the specimen itself. The unstuck electrons, otherwise called secondary electrons, are pulled and collected by positively biased grid or detector, and then translated into a signal to create the SEM image, the electron bar is cleared over the area being inspected created numerous such flays. These signs are then enhanced analyzed, and converted into image, of topography being inspected. Finally, the image or picture is appeared on cathode ray tube (CRT). Fig. 1-8 shows the instrument of SEM.

Fig1-8: Scanning electron microscope (SEM) instrument.

Scanning electron microscope is utilized for inspected topographies of specimen at high amplification. SEM amplifications can go to more than

300,000X. The electrons vitality was set at 10 kv. This was to reduce any harm of test from X-ray radiation [96].

1.10.4 Fourier transforms infra-red spectroscopy (FT-IR)

Fourier transform infrared spectroscopy technique deals with the middle infrared region of the electromagnetic (400-4000 cm^{-1}). Each coavelant bond of organic functions and inorganic species exhibits a characteristic frequency of vibration in FT-IR spectroscopy which can be used to identify its components. The vibration form of molecules is classified in to two types.

1- Stretching vibration (υ) asymmetric and symmetric

2- Bending vibration (δ) in plane (scissoring and rocking), out of pane (wagging and twisting)

Generally, stretching vibration modes are absorption at high frequency than that of binding vibration for same covalent bond.

Absorption a stretch or bend must be changed in dipole moment of the molecule. The asymmetric stretch is usually of higher energy, the energy of stretch decreases as the mass of the atom increases [97].

1.10.5 X-ray photoelectron spectroscopy (XPS)

The technique of X-ray photoelectron spectroscopy, also known as electron spectroscopy chemical analysis (ESCA), was developed by Kai Siegbahn while he was working in Uppsala. Kai Siegbahn was awarded the Noble prize in 1981 for this contribution. The XPS has been considered as one of the major techniques for characterizing/ analysis thin films, solid and surface [98]. The XPS experiment involves bombardment of sample surface with X-ray under-ultra-vacuum (10^{-9} torr). The incident XPS is capable of penetrating many micrometers into the bulk. The atoms in the materials excited by the X-ray lead to ejection of electrons (photoionzation) either from core levels or from valance levels. Electrons generated are prone to scape in to the vacuum in the form of photoelectrons. The overall process is known as the photoelectric effect.In Fig. 1-9 schematic representation of X-ray photoelectron.

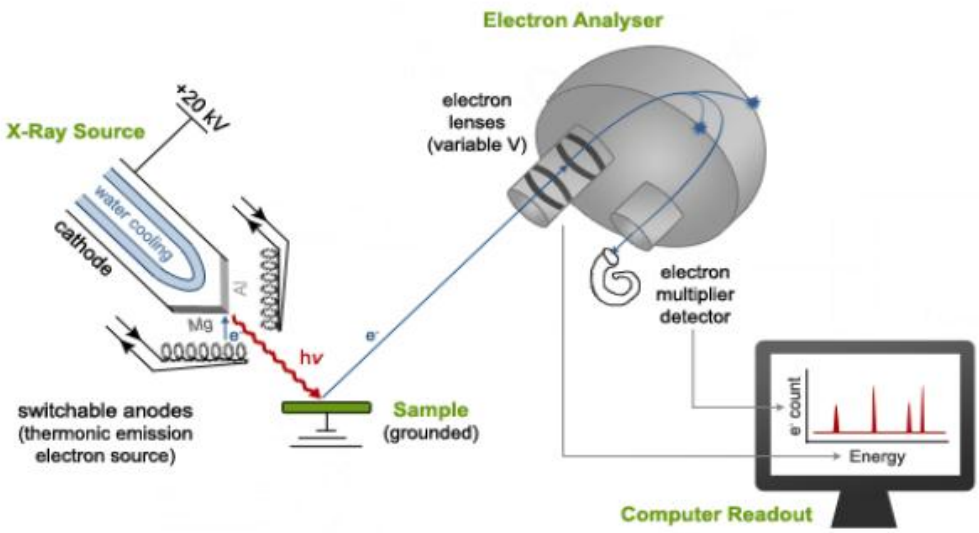

Fig. 1-9: Schematic representation of an X-ray photoelectron spectroscopy

1.10.6 Thermal analysis (TGA/DTG)

Thermal analysis is the analysis of a change in the property of sample, which is related to the imposed change in the temperature. The sample is usually in the solid state and the changes that occur on heating include melting, transition sublimation and decomposition can be analyzed using thermal analysis. The change in the mass of sample and heating is known as thermogravimatric analysis (TGA). TGA calculated change of mass in the substance as a function of temperature under a controlled atmosphere. Its principal uses consist estimated of the substance thermal stability and composition. TGA is most useful decomposition, desorption and oxidation processes. The most widely used thermal method of analysis is [99]. DTG differentia calculation of the weight loss was carried out automatically to give the rate of weight [100]. DTG is the straightforward, it provides reasonably accurate data for most vulcanize and it is faster than the classical extraction method. Fig. 1-9 shows schematic of TGA instrument.

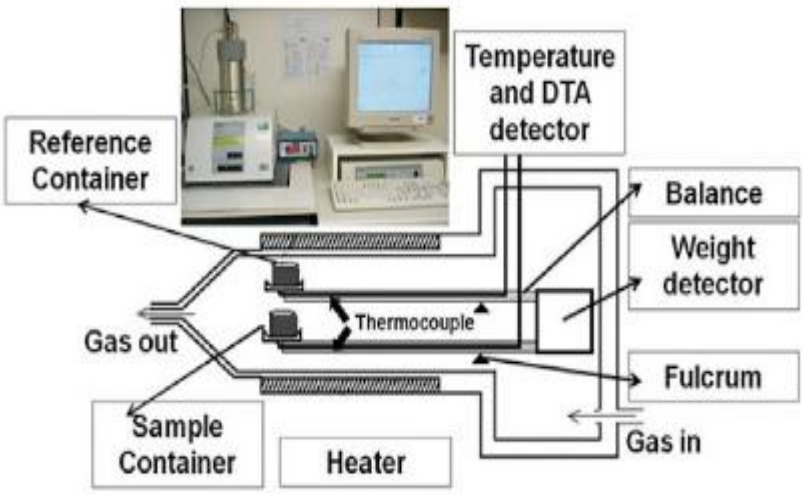

Fig. 1-10: Schematic of TGA instrument

1.11 Aims of the present study

The silica presence in RHA was known since 1983, silica can be extracted via burred the rice husk at 550-800 °C for 6h then synthesis heterogeneous catalyst for hydrolysis important raw material such as cellulose. The main objectives of this work are:

1- Preparation of SiO_2 from rice husk.

2- Immobilized of the silica extracted from RHA with CPTES to synthesis hybrid inorganic- organic material RHACCl than replaced chloro atom with iodo atom to form RHACI then modification with thiourea to synthesis nanoheterogeneous catalyst RHATU-SO_4H.

3- Characterized of new compounds, RHACI and RHATU-SO_4H by using various spectroscopic and microscopic technique such as FT-IR, XRD, SEM, TGA/DTG, XPS and BET (N_2 adsorption-desorption).

4- Studding the cellulose hydrolysis to mono saccharide over synthesis heterogeneous catalyst.

5- Optimization of the catalytic activity of the catalyst.

CHAPTER TWO

Experimental part

2.1 Instruments

All techniques used in this thesis to characterization of compound outside and inside of Iraq were listed below in Table 2-1.

Table 2-1: in this table all companies and places of the analysis were shown.

Technique	Type of apparatus	Place of measurement
FT-IR	Shimadzo-8400s, Japan	Kerbala university/ College of Science
Elemental analysis(CHNS)	Flash EA1112, German	Tehran university/ College of Science
Nitrogen adsorption analysis	nova2000, quantachrome, USA	Sanat Sharif university/ College of Science
SEM analysis	[EDS]-Hidch SU 750, Oxford instruments	Tehran university/ College of Science
Thermal analysis TGA/DTGA	TGA Q50, United Kingdom	Tehran university/ College of Science
X-ray diffraction (XRD)	XRD-6000, Shimadzu	Baghdad university/ College of Education for Pure Science (Ibn Al-Haitham)

UV-Visible	Shimadzu double beam UV-1800 Japan	Kerbala university/ College of Science
pH-meter	WTW(model 720)	Kerbala university/ College of Science
centrifuge	Model EBA-720, Germany	Kerbala university/ College of Science
Balance	AKERM ABS	Kerbala university/ College of Science
Water bath	Lab. Companion BS-11 shaking water	Kerbala university/ College of Science
Oven	Model un-110 plus	Kerbala university/ College of Science
XPS	PECS phoibs 100 analyzer, And SPES X-ray source	UTM University/Malaysia

2.2 Materials

All chemicals are of AR grade, were used directly without further purification. The (RH) was collected from a rice mill in Najaf, Iraq. The chemicals used in this thesis were listed in Table 2-2 below.

Table 2-2: The suppler and purity of all used chemicals.

Item	**Suppler**	**Purity %**
3-Choropropyltriethoxysilane (CPTES)	Sigma, Germany	98
Sodium chloride	GCC, England	99
Acetone	ROML, British	99.7
Benzene	Scharlau	99.5
Cellulose	Merck	98
Dimethylformamide	LOBA. Cheme	99.8
Dimethylsulfoxide	GCC, England	98
Diethylether	CDH, India	96
Ethanol	Sigma eldrge	99
Ethyl acetate	Hi-media, India	98
Lithium chloride	Fluka	99.5
Methanol	GCC, England	98
Nitric acid	CDH, India	70
Potassium iodide	Merck	99.9
Sodium hydroxide	BDH, England	96
Sodium iodide	BDH, England	98
Toluene	GCC, England	98
Triethylamine	CDH, India	98
Thiourea	Sigma, Germany	99

2.3 Preparation

2.3.1 Preparation of rice husk ash (RHA) as a source of silica

Extraction of silica from rice husk (RH) was according to the method reported [101]. In general the RH was washed with water, then rinsed with distilled water and dried at room temperature for 24h. A (30g) sample of the cleaned rice husk was stirred with (750mL of 1.0M) nitric acid at room temperature for 24h, and washed many times with distilled water. The wet material was subsequently dried in room temperature for 24h. It was calcined at 750°C for 6h in a muffle furnace for complete combustion. The white rice husk ash obtained was washed with distilled water and finally it was grind in order to produce a fine powder, which was used as a silica source.

2.3.2 Functionalization of RHA with CPTES

Immobilization of (CPTES) onto RHA has been done according to procedure [102].About 3g of the silica (obtained from RHA) was stirred in (200mL) of 1.0 M NaOH in container of plastic at 80°C for 60 min. The sodium silicate formed was filtrated to remove undissolved particles. The sodium silicate solution of filtrate was used as a precursor for synthesis of catalyst. A (6 mL) of CPTES was added to this solution of sodium silicate. The solution was then titrate slowly (1.0 mL/min) with 3M nitric acid without stirring. The change in pH was monitored by using pH meter. White gel started to form when the pH decreased to less than 11.0. The titration was continued to the pH of the solution reached 3.0. The obtained of gel was aged for 2 days in a covered plastic container. After two days of aging the gel was separated by centrifuge at 4000 rpm for 8 min, the

sparation process was repeated six times with a lot of amount of distilled water. The final rinsing was done with acetone. The sample was then dried at room temperature. Finally, it was ground to produce a fine white powder. This polymer was labeled as RHACCl. The general steps of preparation of RHACCl from the RHA were shown in scheme 2.1.

2.3.3 Iodide-exchange polymer RHACCl

Chloro polymer RHACCl (1g) was mixed in dry acetone (50 mL) containing NaI (4g) and the mixture refluxed at 70°C for 60h. The produced was then filtered off, washed with water many times, methanol and ether and dried in oven at 100°C for 24h [103]. This iodo polymer (0.85g) have white color was labeled as RHACI.

2.3.4 Synthesis of silica – Thiourea catalyst (RHATU-SO_4H)

Thiourea (TU) 2g (0.026mmol) was dissolve in dry toluene (30mL) containing RHACI (1g) and Et_3N (3.79mL, 0.026mmol) and the mixture refluxed at 110°C for 24h. The product was filtered and washed with DMSO, ethanol and methanol. The product dried at 110°C for 24h. This was a sample labeled as RHATU. After that 40 mL of 0.5M sulfuric acid was stirred with (2.0 g) RHATU at room temperature for 24h, the solid has been washed and filtrated with copious distilled water and dried in oven at 110°C for 24h [51]. Finally, (0.85g) result white powder the product compound was labeled as RHATU-SO_4H.

2.3.5 Cation exchange capacity of the catalyst (CEC)

Cation exchange capacity (CEC) was done depending on the described method[104], (1.0 g) of RHATU-SO_4H that was mixed with (1.0g) of sodium chloride that dissolved in 25mL distilled water in conical flask with magnetic stirrer for 30min. Then added (2-3) drop of phenolphthalein indicator (1%, 0.1 g from indicator soluble in 50mL of ethanol, and complete the solution to (100mL) with distilled water) to mixture and the sample titrated with standard sodium hydroxide (1.0M) solution. This process repeated three times titration was perform to contained average value for the cation exchange capacity of RHATU-SO_4H.

2.4 Catalyst reaction

2.4.1 Cellulose hydrolysis

Hydrolysis of the cellulose was carried out in a liquid-phase reaction in a (250mL) round bottom flask with water condenser and magnetic stirrer. 30mL of DMF, LiCl (0.2g) and cellulose (0.18g) were individually transferred to the round bottom flask containing the catalyst (per- dried at 110°C for 24h and cooled in a desiccator to minimize moisture content). The temperature of the reaction fixed at 140°C, a mixture of the reaction was refluxed for 16h [105].

2.4.2 Determination of glucose concentration produced from hydrolysis of cellulose

In order to estimate the concentration of the produced glucose from hydrolysis of celluloses, 3,5-dinitrosalicylic acid (DNS) method was used in which the aldehyde group of glucose converts DNS to its reduction from 3- amino-5-nitrosaliclic acid. The amount of 3-amino-5-nitrosalicylic acid

formed is proportional to the amount of glucose. The synthesis of 3-amino-5-nitrosalicylic acid leads to a change in the amount of light absorbed, at wavelength 540 nm [106].

2.4.3 Glucose standard curve

A series dilution of stock solution (0.2, 0.4, 0.6, 0.8, 1.0 and 1.2 mg/mL of glucose) were prepared in 10mL using distilled water.

A (0.5mL) portion of the hydrolyte solution from the mixture of reaction was transferred to the avail and 2.0 mL of sodium hydroxide (2N) and (2.0 mL) reagent of the DNS were added and the reaction mixture was incubated in a water bath at boiling point for 10min. The reagent plank sample was with 0.5ml of DNS reagent and (2mL) of deionization water and heated at the same condition of the sample. Then absorption was measured at 540nm, against a reagent blank (the color of the solution was yellow at the start and would be red with increasing of cellulose hydrolysis). The concentration of glucose in solutions was estimated by the employing a standard curve prepared using glucose. Fig. 2-1 shows standard curve of glucose

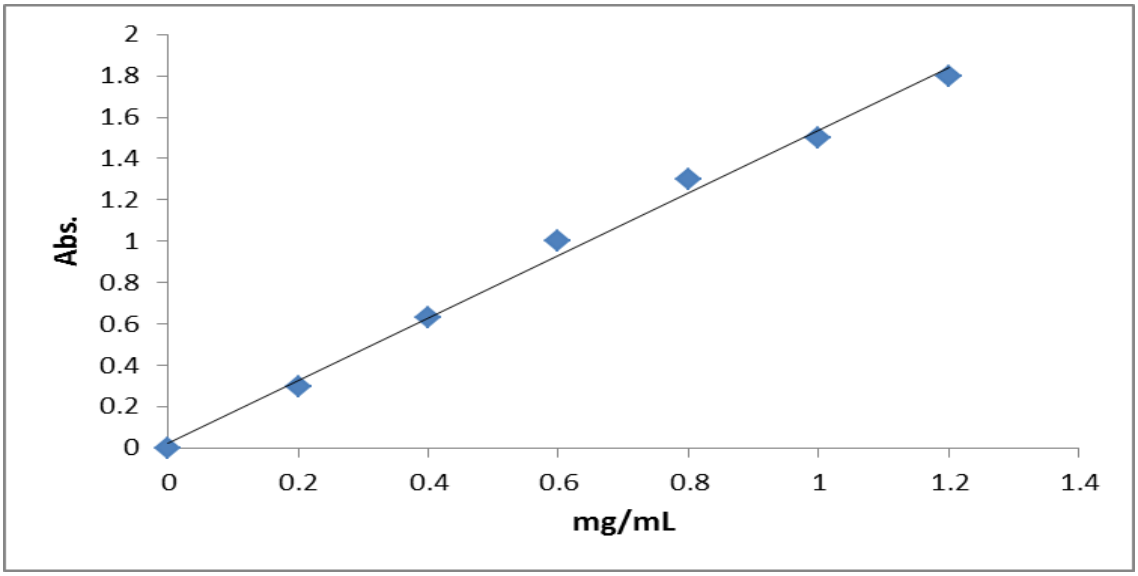

Fig. 2-1: Standard curve of glucose.

2.4.4 The optimization of the catalyst mass

The activity of catalyst with different catalyst mass (150,200 and 250mg) was studied by following the same procedure as in section 2.4.3. The temperature of reaction was carried out at 140°C for 16h.

2.4.5 The optimization of reaction temperature

The catalyst effected at different temperature (120,130 and 140°C) was studied by using same procedure as in section 2.4.3 the hydrolysis of cellulose was carried out using (0.2g) of the catalyst for 16h.

2.4.6 The solvent effect

The activity of catalyst was studied with different solvents (toluene, 2-methyl propanol, and DMF). It was studied using the same procedure as in section 2.4.3. The hydrolysis reaction was carried out at 140°C for 16h.

2.4.7 The reusability of the catalysts

To check catalyst s' reusability experiment was conducted by running the successively the hydrolysis with the same catalyst under the same hydrolysis condition. The hydrolysis was first run using fresh catalyst to complete conversion. The catalyst was filtered and washed with absolute ethanol and dried at 110°C. After these steps, the catalysts were reused under optimized reaction condition.

2.4.8 Hydrolysis procedure using homogenous catalyst

For comparison, the cellulose hydrolysis using homogenous catalyst was studied with thiourea. Typically, a (250mL) capacity three necked round-bottom flasks, equipped with water condenser and magnetic stirrer were used. (30mL) of DMF was added to into the round –bottom flask containing (0.18g) of cellulose (0.2g) of lithium chloride and (0.2 g) from thiourea. The hydrolysis of mixture refluxed for 16h at 140°C the concentration of glucose monitoring according to procedure in section 2.4.3.

2.4.9 Hydrolysis of cellulose from different source

Hydrolysis of cellulose from sunflower and paper was carried out in a liquid-phase reaction in a (250mL) round bottom flask with water condenser and magnetic stirrer. (30mL) DMF, LiCl (0.2g) and cellulose (0.18 g) were individually transferred to the round bottom flask containing the catalyst (per- dried at 110°C for 24h and cooled in a desiccator to minimize moisture content). The temperature of the reaction fixed at 140°C, a mixture of the reaction was refluxed for 16h.

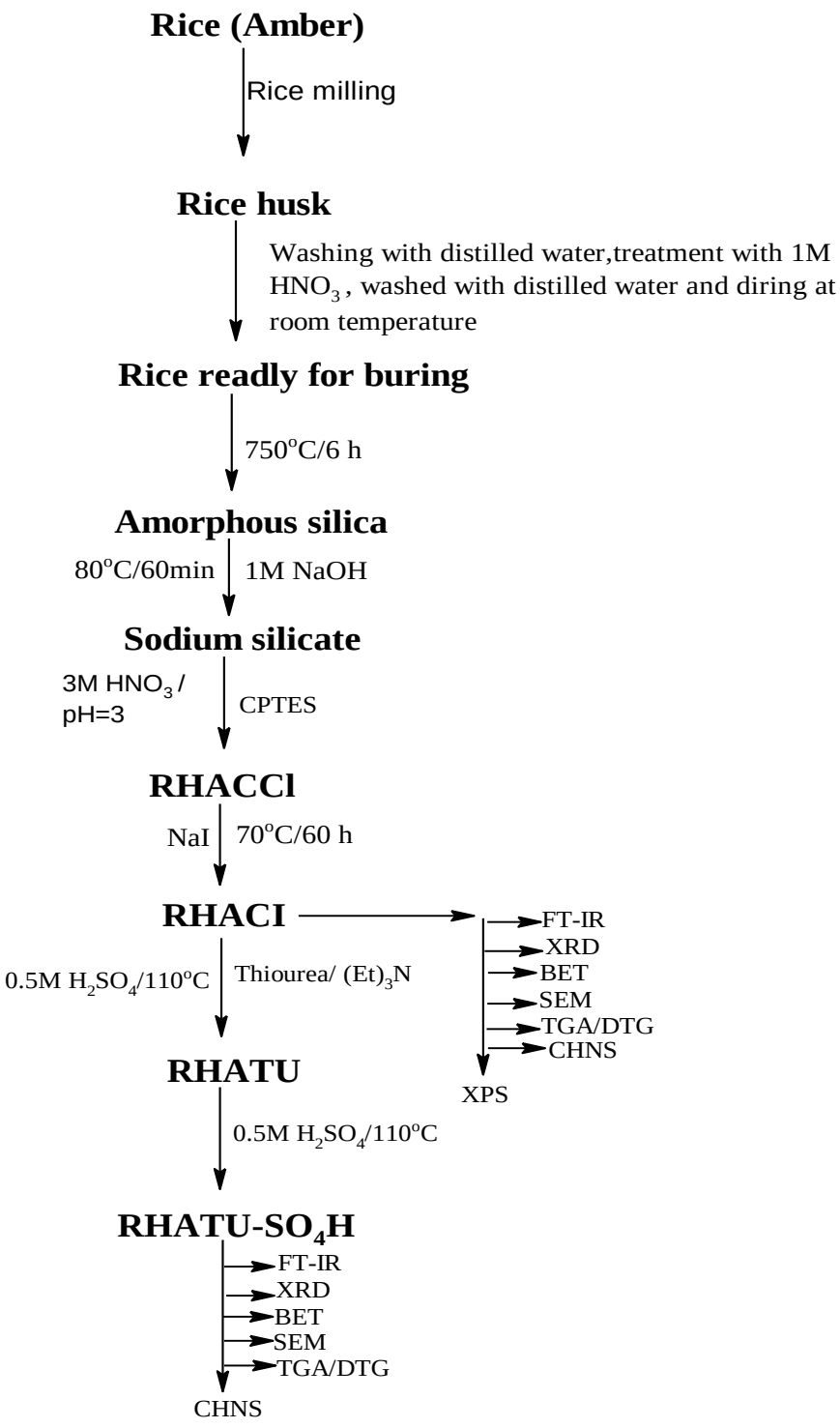

Scheme 2-1: Research progress during the catalyst synthesis.

CHAPTER THREE

The characterization of RHACI and RHATU-SO_4H

3.1 Introduction

In this regard, 3-chloropropyltriethoxysailine (CPTES) was immobilized on silica extracted from RHA at a short time (60 min). Modified silica by processes of sol-gel had been synthesized through reaction between silylating agents bearing and functional groups sodium silicate in water as a solvent. After sol-gel reaction is completed, the functional groups are attached onto the silica matrix by stable Si-C bonds. The chloro group in RHACCl was replaced in iodo group to form RHACI; through added NaI in acetone at 70 °C for 60h. Thiourea was immobilized on RHACI to synthesize nanoheterogeneous catalyst labeled RHATU-SO_4H.

3.2 Characterization of RHACI

The RHACI was prepared by the replacement reaction of chloride group from RHACCl with iodo group from NaI, scheme 3-1 shows the prepared RHACI.

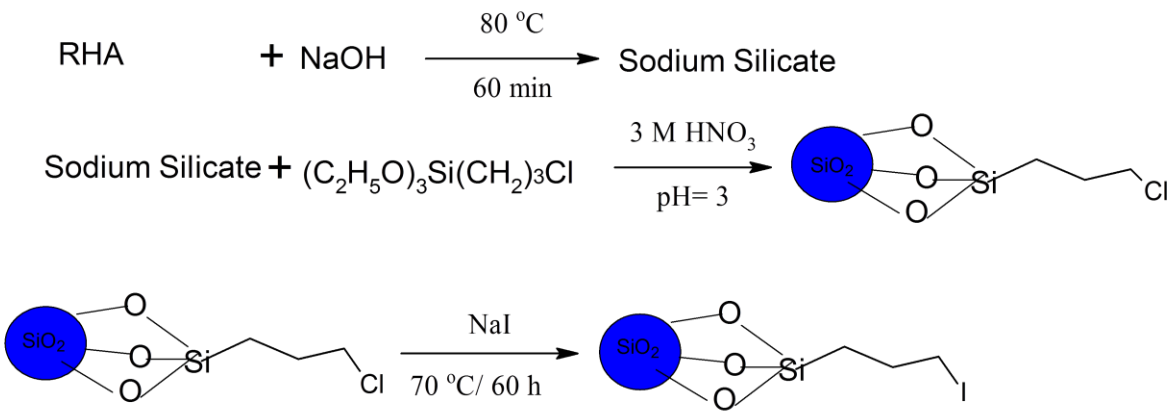

Scheme 3-1: Preparation of RHACI

3.2.1 Fourier transformed infrared (FT-IR) spectroscopy

FT-IR spectra of RHACI and RHACCl are shown in Fig. 3-1 the broad band at 3556 -3553cm^{-1} is usually assigned to the stretching vibration of SiO-H bond and H_2O adsorbed on the surface of silica. The band at 1056.20 cm^{-1} was assigned to the asymmetric stretching vibration of Si-O-Si bonds [107]. A band at 802 and 462-428 cm^{-1} were assigned to symmetric stretching and bending of bulk Si-O-Si bond respectively. The band absorbed at 954.8cm^{-1} was assigned to stretching vibration of Si-OH the surface silanol groups [108].

FT-IR spectrum of the RHACCl appearance absorption bands at 696 cm^{-1} assigned to C-Cl bond, while this band disappeared in the spectrum of RHACI, and appearance new band in the spectrum of RHACI at 580 cm^{-1} assigned to stretching vibration of $–CH_2$-I [109]. The appearance band C-I and disappearance of C-Cl band are good evidence to synthesis of RHACI.

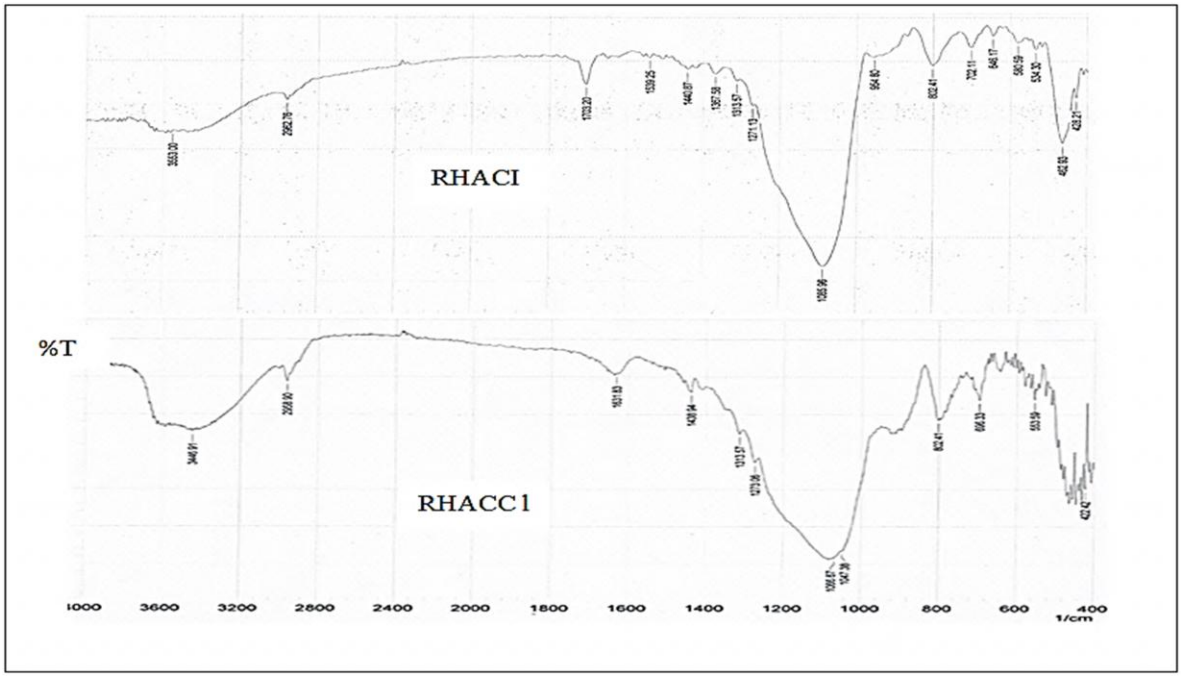

Fig. 3-1: FT-IR spectra of RHACI and RHACCl

3.2.2 X-ray diffraction (XRD) pattern

The X-ray diffraction pattern spectrum of RHACI is shown in Fig. 3-2 the created silica appears broad peak at 2θ = 22° which is an indication of the amorphous nature of RHACI [110]. No Absorbance of any structure of crystalline can be seen by lack of sharp peaks.

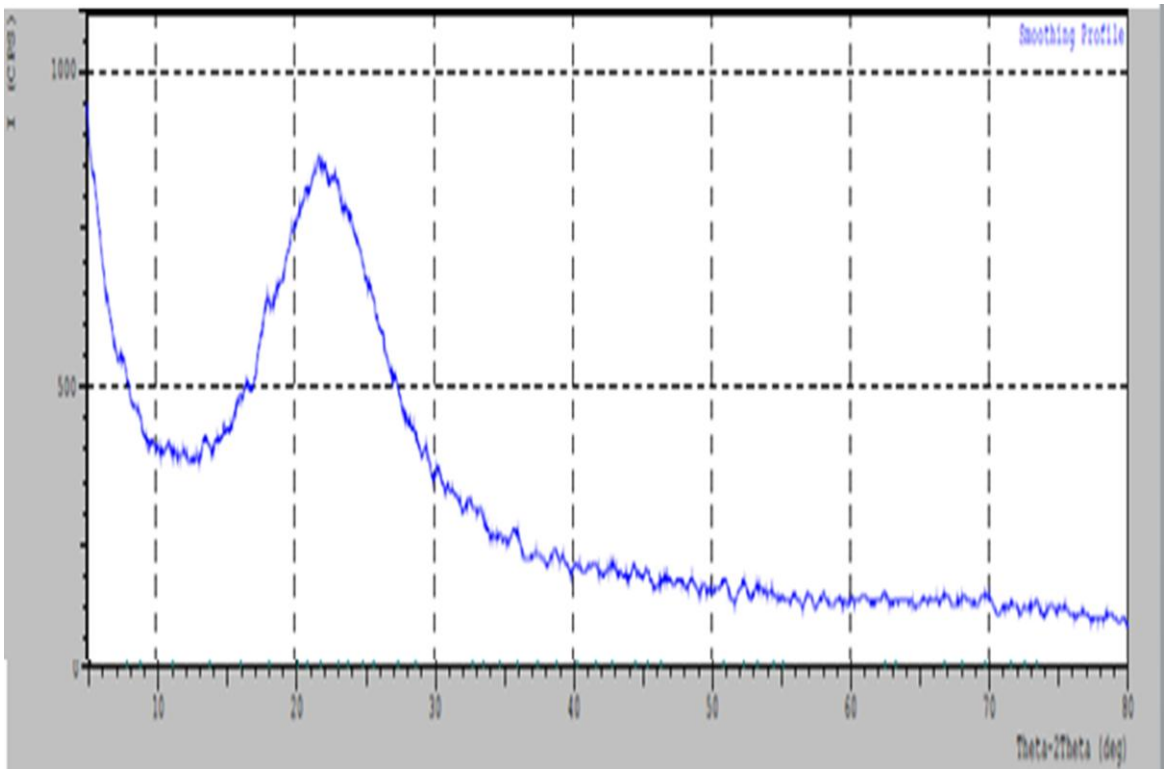

Fig. 3-2: X-ray diffraction pattern for RHACI.

3.2.3 Thermal analysis TGA/DTG of RHACI

Fig. 3-3 shows the thermogravimetric analysis result for RHACI substance with rising temperature has two stages of weight loss. First weight loss is (ca. 2.482%) at temperature from (26.68-130)°C assigned to the loss physical/chemical of water adsorbed onto silica surface [111]. The second stage of weight loss (ca. 28.09%) at (130-590)°C attributed to decomposition of organic moiety (iodopropyl) that associated with silica.

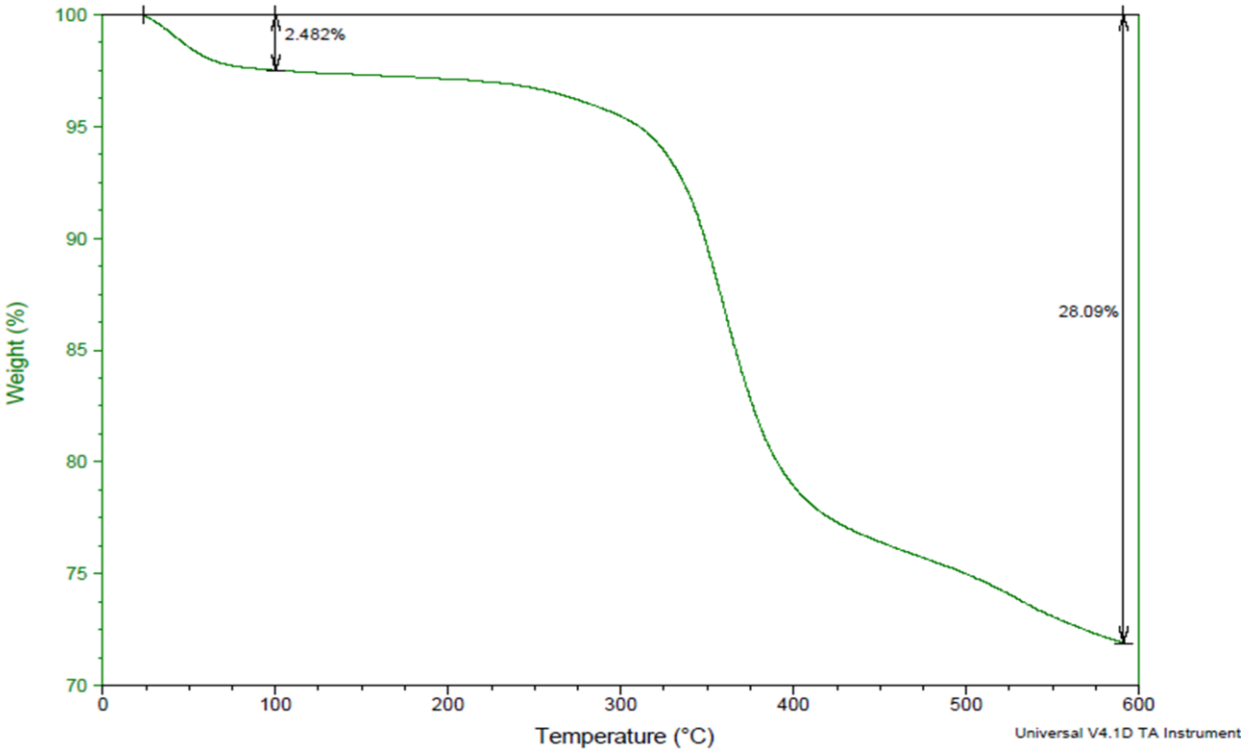

Fig. 3-3: Thermal analysis (TGA) of RHACI

The DTG analysis for RHACI showed in Fig. 3-4, the thermal degradation of RHACI has two main decomposition stages. The first loss of weight loss (ca. 2.482%) about (26.68 -130) °C at maximum temperature (44.43°C) assigned to loss the adsorbed of water on the silica surface. The

second weight loss between (130-470)°C has maximum temperature 359.12°C attributed to loss weight organic groups (iodopropyl). Third stage at 490-580°C has maximum temperature 530.92°C assigned to loss of silanol condensation on silica surface [52]. This clearly shows the successful replacement chloride group by iodo group to form RHACI.

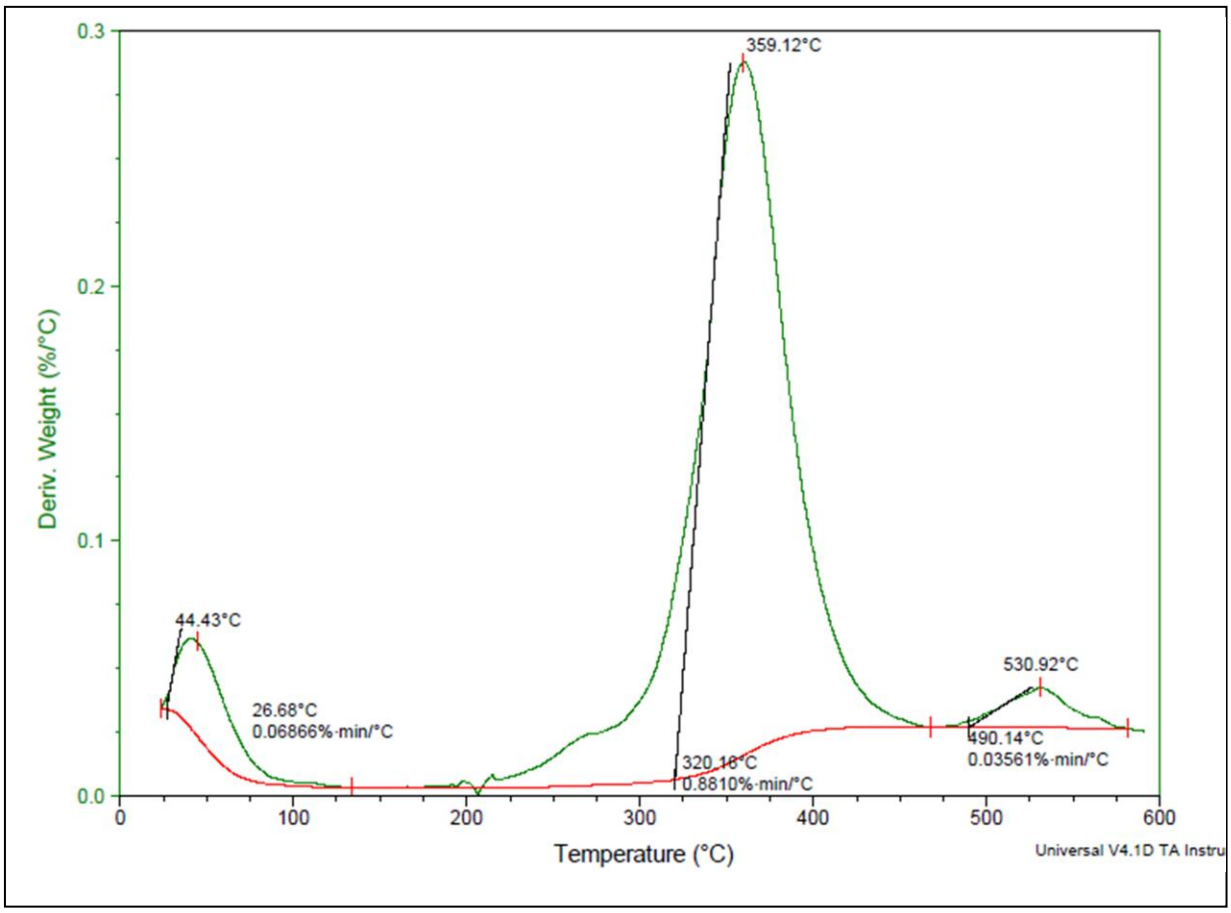

Fig. 3-4: Thermal analysis (DTG) for RHACI.

3.2.4 The scanning electron microscope (SEM) of RHACI

The SEM morphology of RHACI powder was shown in Fig. 3-5. The particles were irregular and agglomerated in character. The shape of RHACI particles like to a shell or rocky shape [112].

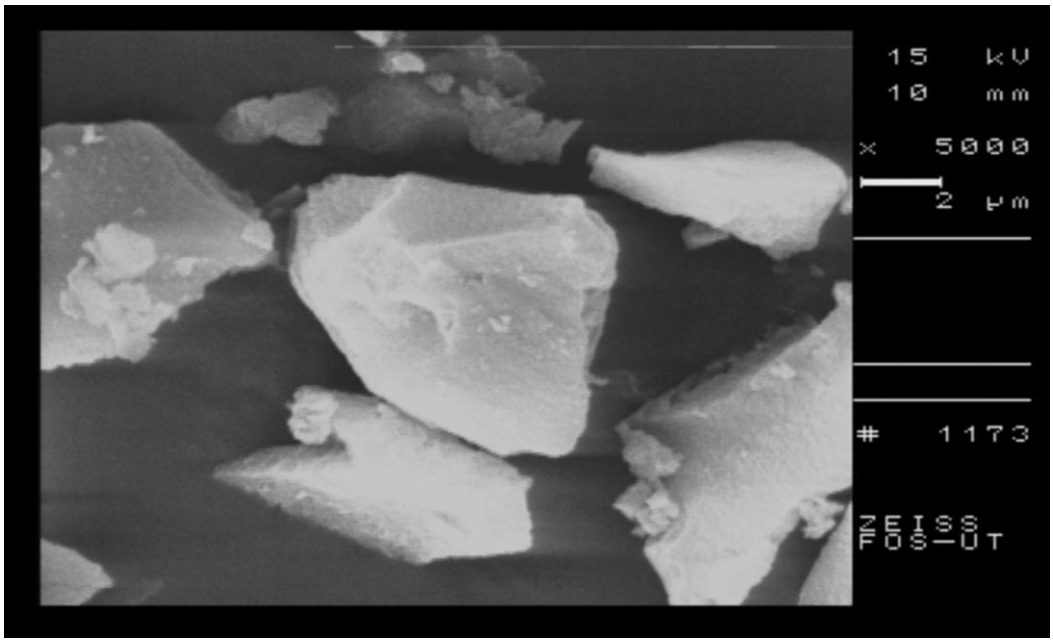

Fig.3-5: SEM morphology of RHACI powder

3.2.5 The nitrogen adsorption desorption

Fig. 3-6 shows the BET adsorption-desorption isotherm obtained for RHACI. The hysteresis loop shown in the range around $0.4<p/p^{\circ}<1.0$ which was related with capillary condensation taking place within the mesopores [102]. This appears the presence of mesoporous holes in the RHACI material. According to the IUPAC classification, the isotherm shows type IV and exhibited on H2 hysteresis loop [113]. The BET analysis showed the specific area of RHACI 410 $m^2 . g^{-1}$, while the specific surface

area of RHACCl was 633 $m^2 g^{-1}$. The decreased in specific area of RHACI, however, could due to the reduction of surface of sites to replace a large size of iodo molecule causing the surface to be over crowded with the ligand network on the surface and blocking the pores. The RHACI was showed narrow pore size range from (2.2-11.7) nm within range of mesoporous. A result obtained by BET N_2 adsorption-desorption analysis of RHA, RHACCl and RHACI summarized in Table 3-1.

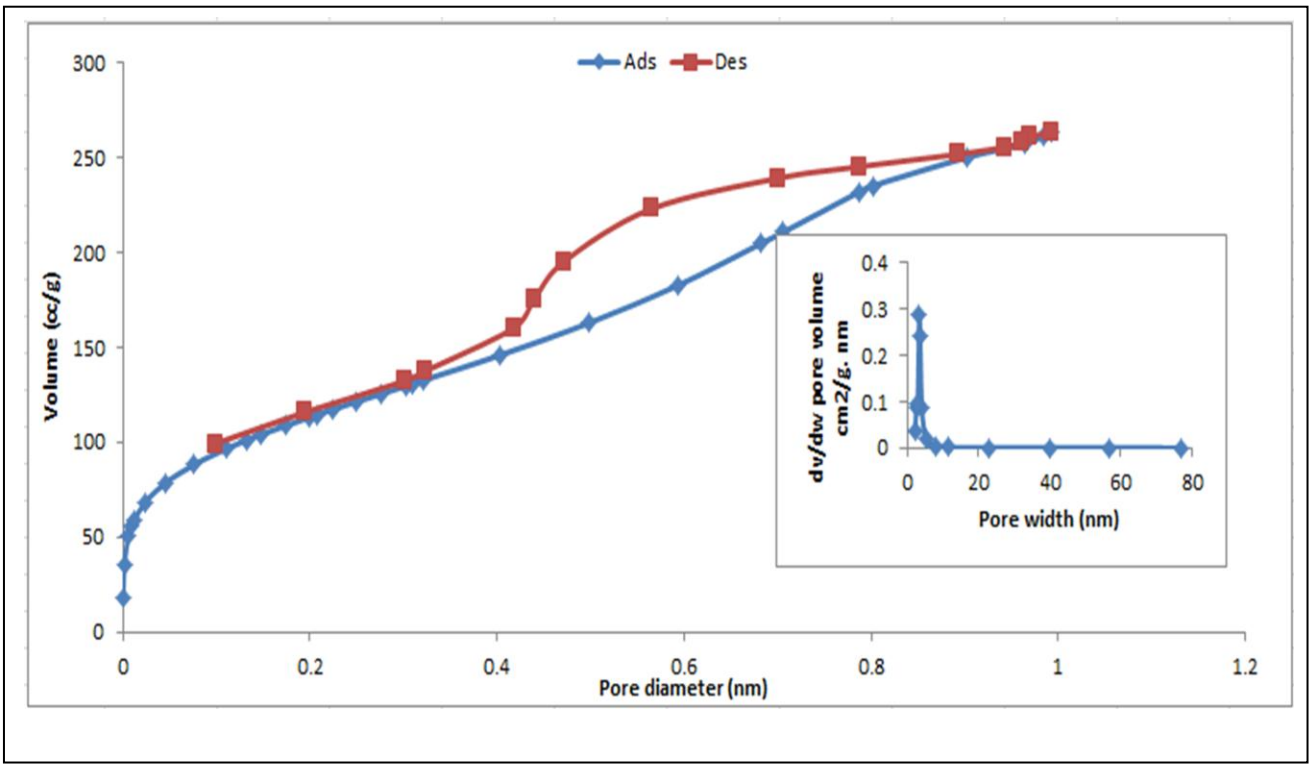

Fig. 3-6: N_2 adsorption-desorption for RHACI.

Table 3-1: shows result of BET analysis for RHACI, RHA and RHACCl.

Sample	Specific surface area m^2/g	Average pore volume cm^3/g	Average pore diameter (nm)	Ref.
RHA	347	0.87	10.4	[101]
RHACCl	633	0.705	6.07	[102]
RHACI	410	0.396	3.86	…….

3.2.6 X-ray photoelectron spectroscopy (XPS)

X-ray photoelectron spectroscopy is a sensitive quantitative spectroscopic technique that can be used to characterize the surface of sample and identify all the elements present in the top layer of substance. High sensitive of XPS for surface (typical sampling depths of 1-2nm) one of the maximum powerful broaches for both qualitative and quantitative properties of surface [114]. XPS is used to study the binding energy of core level electrons in an atom and changes in the binding energy due to the atoms being in different chemical environments. XPS also provides information of the surface chemical composition and the chemical state of the elements in a sample [115].

The elemental composition of the surface was assessed by XPS. The results in Fig. 3-7 clearly showed that after the RHACCl treatment with iodide, the chloride content decreases (3.3%) and the iodide increases (30%). The percent elemental composition for chloride and iodide were calculated by dividing the intensity of the elemental line by the sum of the intensities of the elemental lines observed for the specimen [116].

The XPS spectrum of the Si 2p Fig. 3-8 shows a peak at ca. (101.5)ev binding energy [117]. The Fig.3-9 O 1S BE was found at (531.0) ev for RHACI [118]. The XPS spectra of I 3d for all the studied surfaces are presented in Fig. 3-10 the peaks located at 618.5 eV and 630 eV binding energies are associated with C–I and NaI bonds, respectively [119]. The XPS spectrum of the C 1s Fig. 3-11 shows a peak at ca. (284) ev is associated to C-Si and C-H [120]. The XPS also appear a peak at (199) ev is associated to Cl 2p that residue from replacement process or that not replacement in CPTES [121]. Then XPS has also indicated peak at ca. (1070) ev linked with of Na is species, the presence of Na is due to the

replacement process of the chloro group by iodide group (NaI) [122]. It can clear from XPS seen in Fig. 3-7 that there is (Cl) atom content in RHACI very small compared with high concentration of iodide atom. The XPS produces good evidence to successful replacement process to form RHACI.

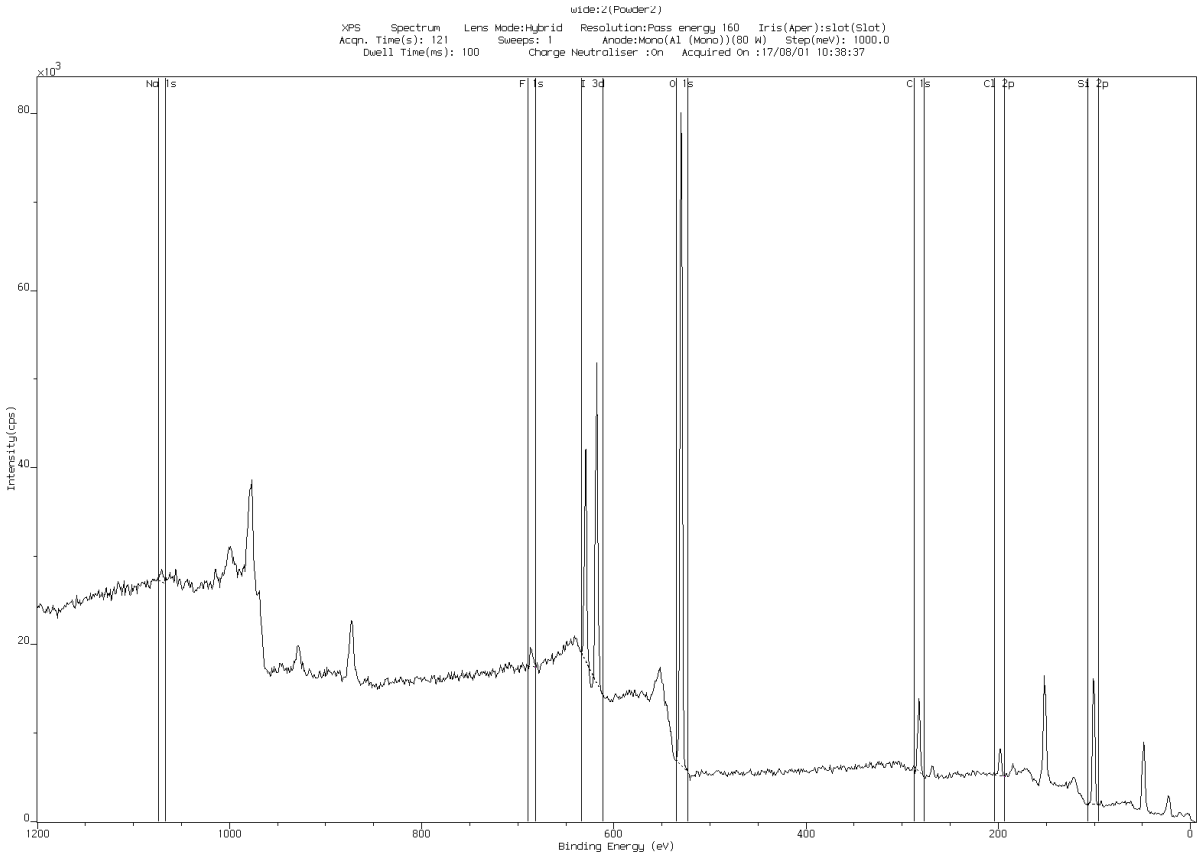

Fig. 3-7: XPS spectrum of RHACI shows content the C, O, Si, Cl and I.

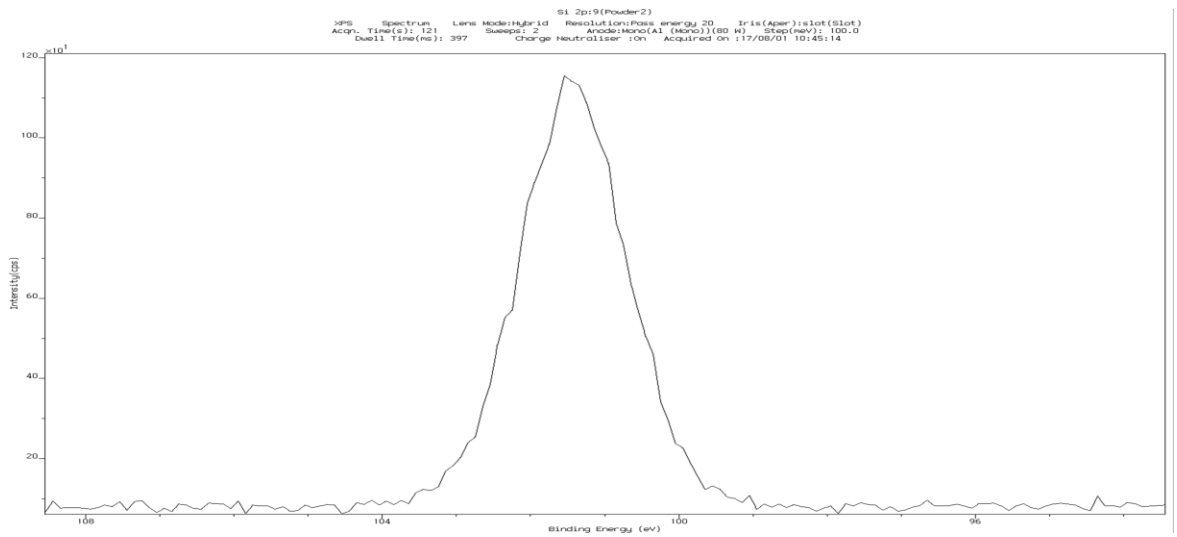

Fig. 3-8: XPS spectrum of Si 2p from RHACI.

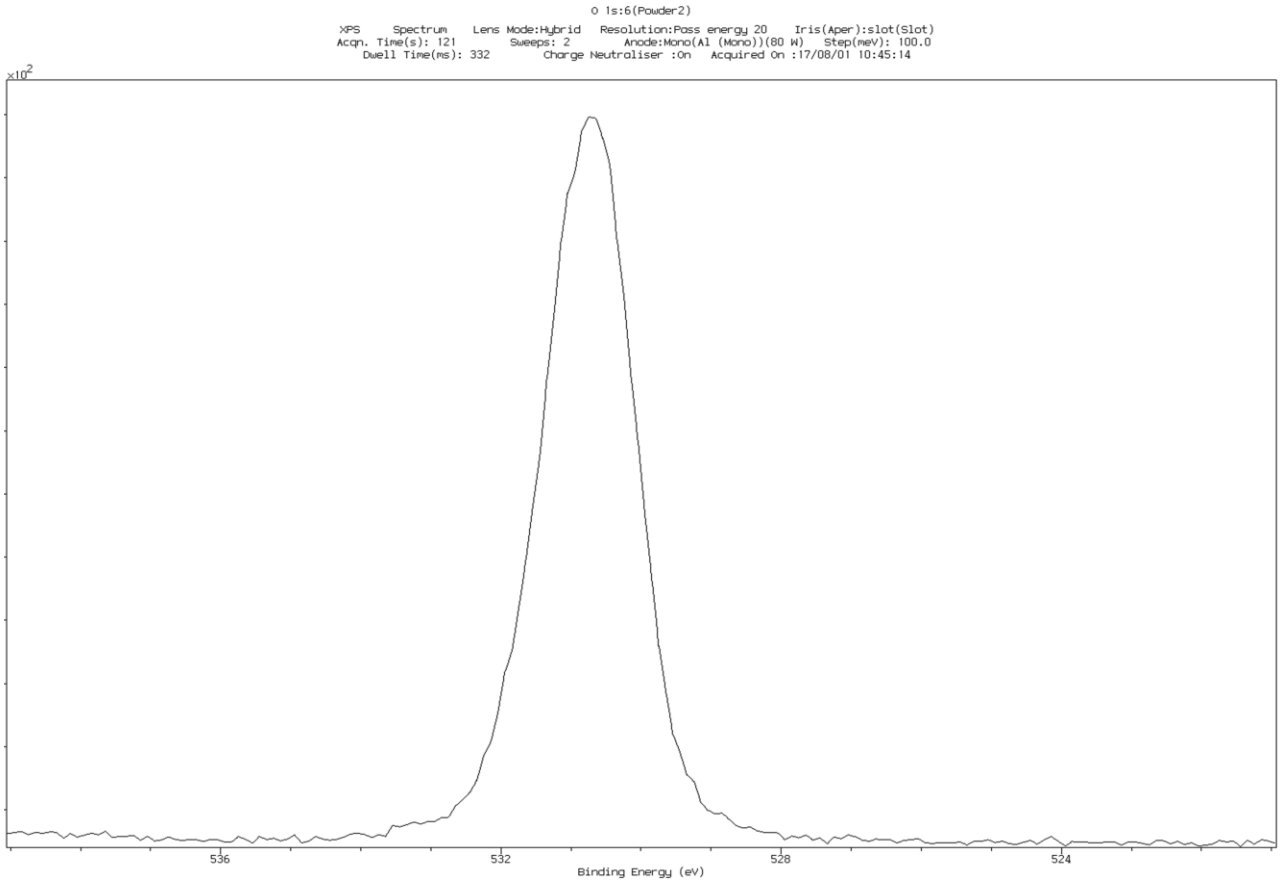

Fig.3-9: XPS spectrum of O 1S from RHACI.

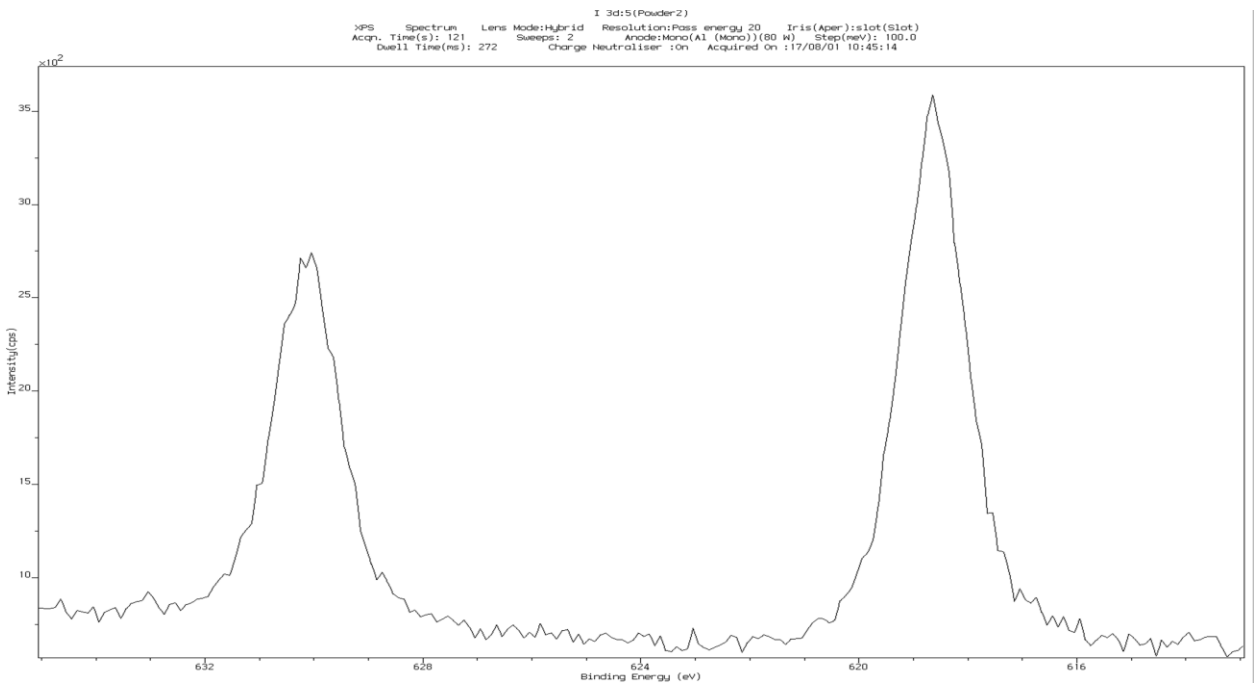

Fig. 3-10: The XPS spectrum of I 3d from RHACI and NaI.

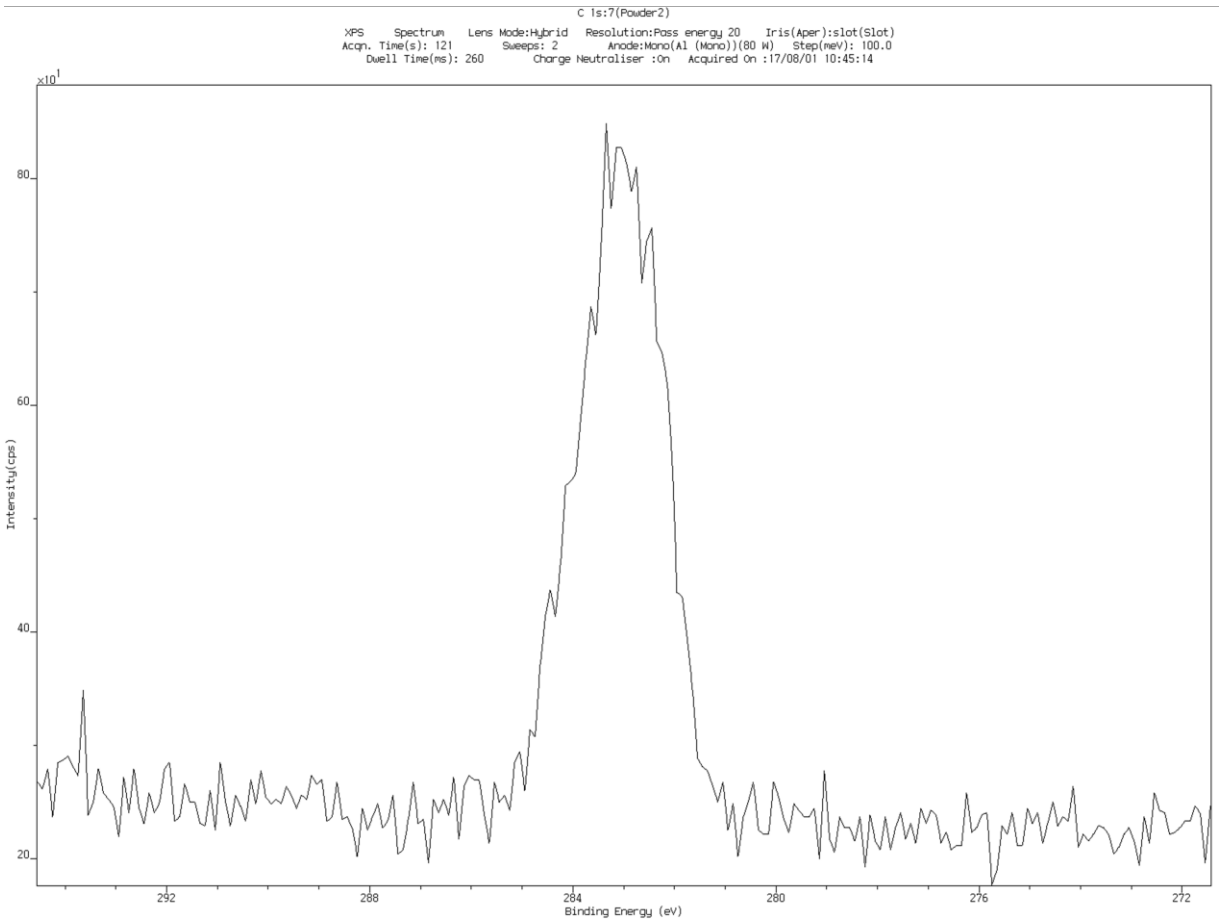

Fig. 3-11: The XPS spectrum of C 1s from RHACI.

3.3 The characterization of silica – Thiourea, RHATU-SO_4H

The immobilization of thiourea (TU) to RHACI was carried out in a heterogeneous reaction. In the heterogeneous reaction one or more of the reactant could be in different state. In this reaction the dry toluene was used as solvent and the mixture of reaction was refluxed at 110 for 24h, yielding the products as shown in scheme3-2.

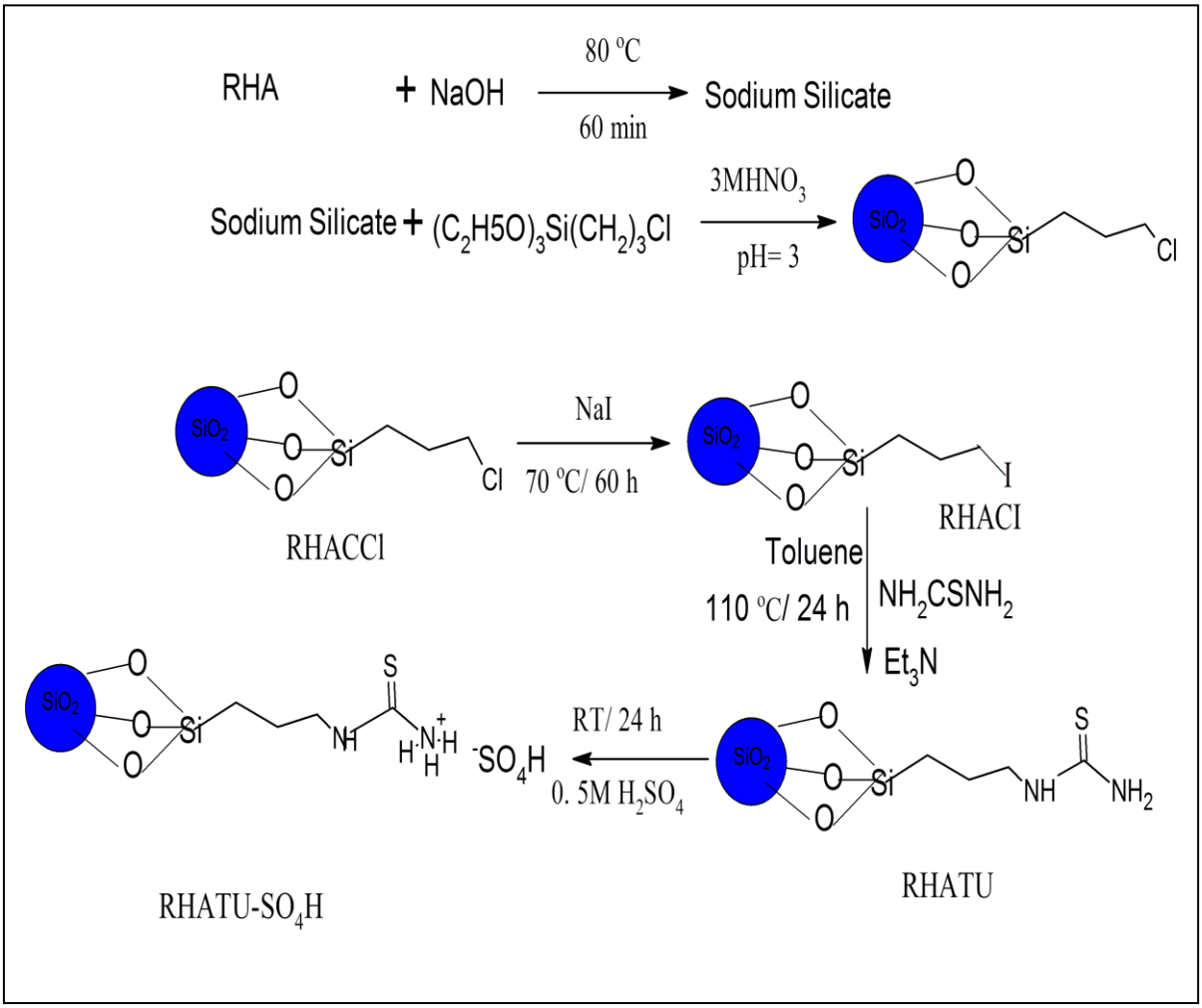

Scheme 3-2: Synthesis reaction of RHATU-SO_4H.

3.3.1 The FT-IR spectrum of RHATU-SO_4H

Fig. 3-12 shows the FT-IR spectra of RHATUSO_4H and RHACI. The strong broad band absorption at 3412 cm^{-1} attributed to stretching vibration of –O-H onto the surface of silica and H_2O adsorbed onto the surface of silica. The stretching vibration absorption at 1084 cm^{-1} assigned to (Si-O-Si) in catalyst. The stretching vibration at 2929cm^{-1} attributed to aliphatic -CH_2 [123]. Observation asymmetric stretching vibration at 1541 cm^{-1} assigned to N-C-N from catalyst [124].

Stretching vibration band at 3188 cm^{-1} assigned to $^{+}NH_3$ [125]. The stretching vibration band at 3325cm^{-1} attributed to secondary amine N-H [126]. The bending vibration of H-O-H was observed at 1618 cm^{-1} [8]. The stretching vibration of sulfate O=S=O bonds was shown at 1402 cm^{-1}. At 1456 cm^{-1} is observed a band assigned to N–H bend of secondary amines [127]. This information is good evidence to formation of RHATU-SO_4H catalyst.

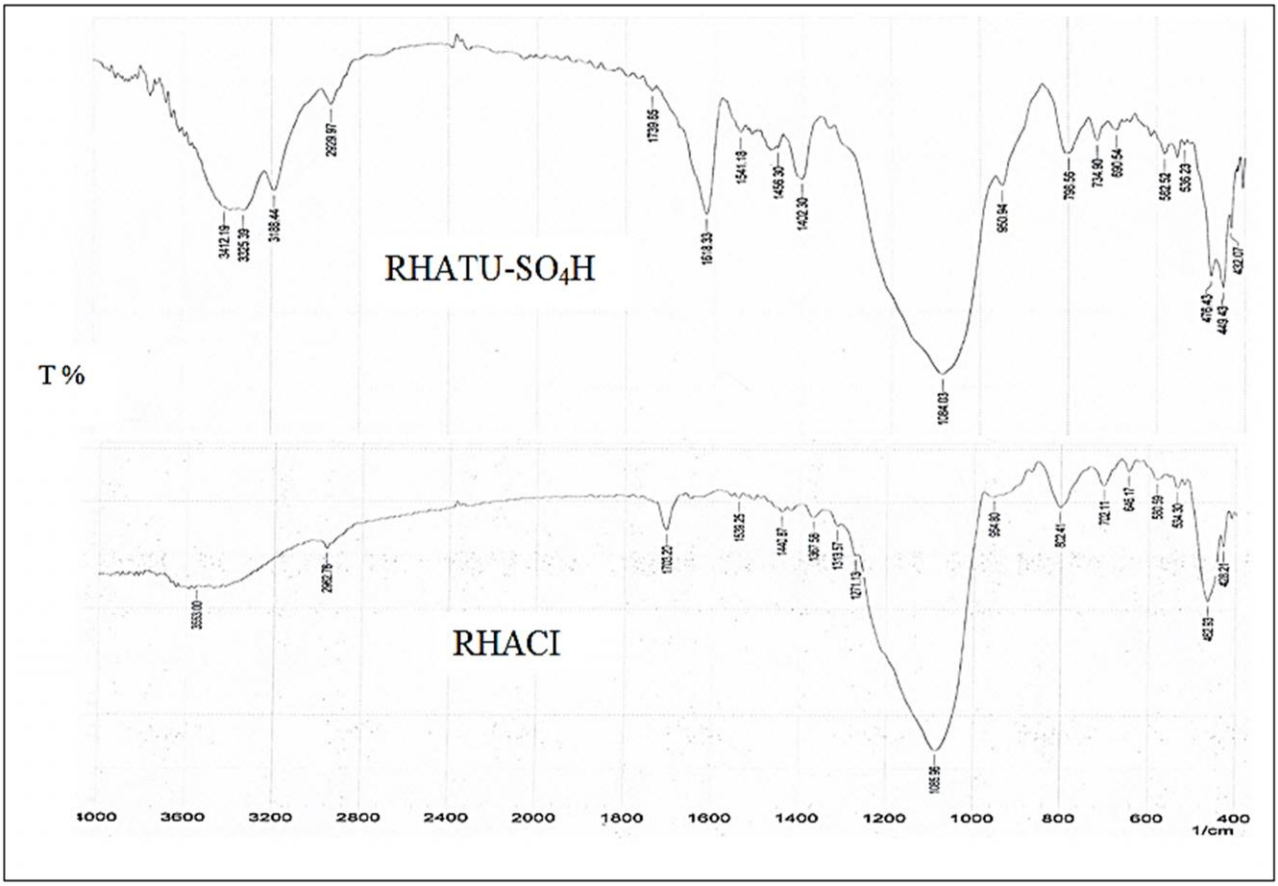

Fig. 3-12: FT-IR spectrum for RHATU-SO_4H.

3.3.2 Powder X-ray diffraction (XRD)

Fig. 3-13, shows XRD pattern of RHATU-SO_4H catalyst. It was noted there is no sharp peak appear for crystalline form this indicates that catalyst RHATU-SO4H is amorphous that gives broad peak at

$2\theta = 22^{\circ}$. However, no change in catalyst phase after the thiourea immobilized onto RHACI.

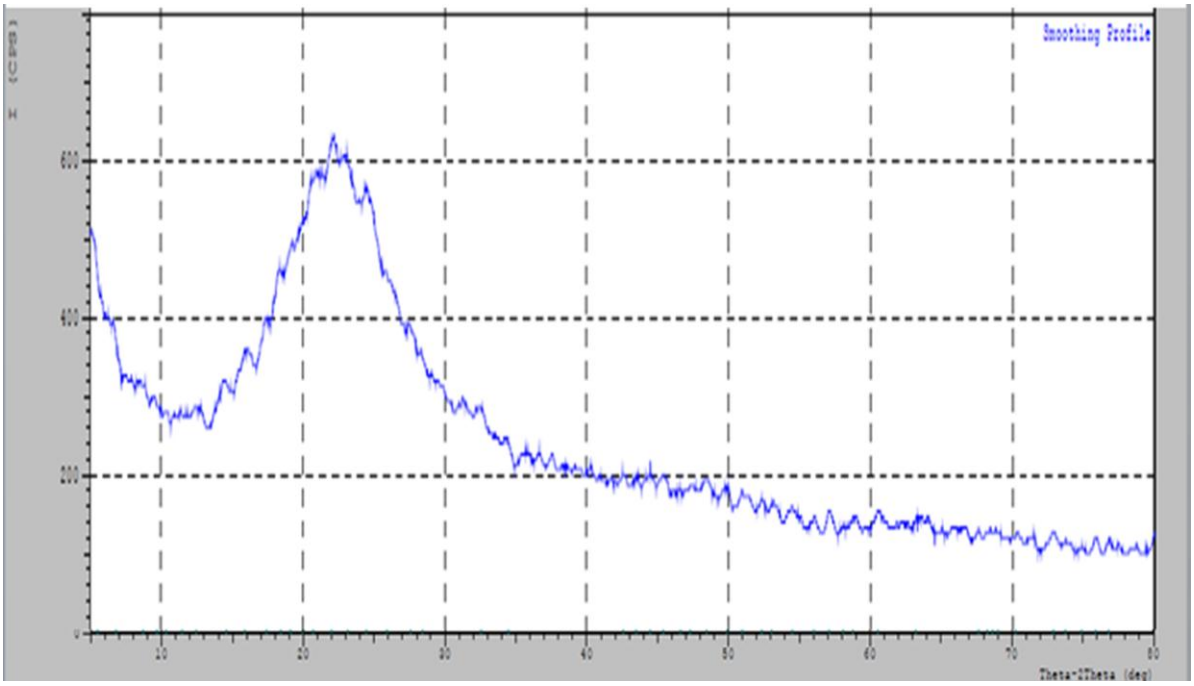

Fig. 3-13: X-ray diffraction pattern of RHATU-SO_4H.

3.3.3 Elemental analysis

Elemental characterization of RHATU-SO_4H samples was performed by CHNS- analyzer to determine the percentage amount of carbon, hydrogen, nitrogen and sulfur present in RHATU-SO_4H. Carbon content found greater than these in RHACI. The elemental analysis for RHATU-SO_4H is showed the percentage of carbon, hydrogen, nitrogen and sulfur (13.18%, 2.96%, 1.44% and 8.94%) respectively. Nitrogen and sulfur are not shown in both RHACI and RHA (Table 3.2) from the elemental analysis results clearly indicate that the thiourea was successfully immobilized onto RHACI.

Table 3-2: shows the elemental analysis for RHA, RHACI and RHATU-SO_4H.

Sample	%C	%H	%N	%S
RHA	1.6	0.84	……..	……..
RHACI	9.98	1.61	……	……..
$RHATUSO_4H$	13.18	2.96	1.44	8.94

3.3.4 The determination of percentage loading of organic ligands

The molar amount of grafted organic phase per gram silica (M) can be calculated according to method reported in reference [24]. The molar amount of grafted organic phase onto silica (M) calculated according to the equation.

$$M(\mu\, mol\ g^{-1}) = \frac{10^6\left(\frac{P_C}{100}\right)}{12n}$$

Where Pc is the presence of the carbon element dependent to the elemental analysis and n is number of carbon atoms per organic molecule. On the other hand, the weight percentage of the grafted phase (Pw) can be calculated form the equation.

$$P_w = m \times 10^{-4} M$$

Where m is the molecular mass of each molecule of organic grafted. The surface converge (N) can be calculated as from.

$$N(M\ mol\ m^{-2}) = \frac{M}{\left\{S\left[\frac{(100-P_w)}{100}\right]\right\}}$$

$$= \frac{10^6\ P_c}{12nS(100-P_w)}$$

Where S is the coverage of the surface area per 1.0 g of non-modified silica. Using this equation to calculated of grafting amount of thiourea on RHAC-I was found to be 83.605%. The coverage of surface N (µmol m^{-2}) per 1.0 gram silica was found to be 187.55 µ mole m^{-2}.

3.3.5 The nitrogen adsorption analysis

The surface analysis of RHATU-SO_4H was determined by the nitrogen adsorption-desorption, Fig. 3-14, shows the N_2 adsorption-desorption isotherm and EJH distribution of pore size for RHATU-SO_4H. IUPAC classification of the isotherm for RHATU-SO_4H agrees with the type IV and H2 hysteresis loop [128]. The nitrogen adsorption isotherm obtained for RHATU-SO_4H gave a hysteresis loop observed in the range of $0.4 < P/Po < 1.0$; this is associated with capillary condensation according to IUPAC classification. The BET analysis showed that the specific surface area of the RHATU-SO_4H was 357m^2/g while specific surface area of RHACI was 410 m^2/g. A decrease in the surface area of the RHATU-SO_4H could be due to the immobilization of thiourea on the silica surface which causing block in some the pores. RHATU-SO_4H has pore size distribution (2-20nm) which falls within the mesoporous region.

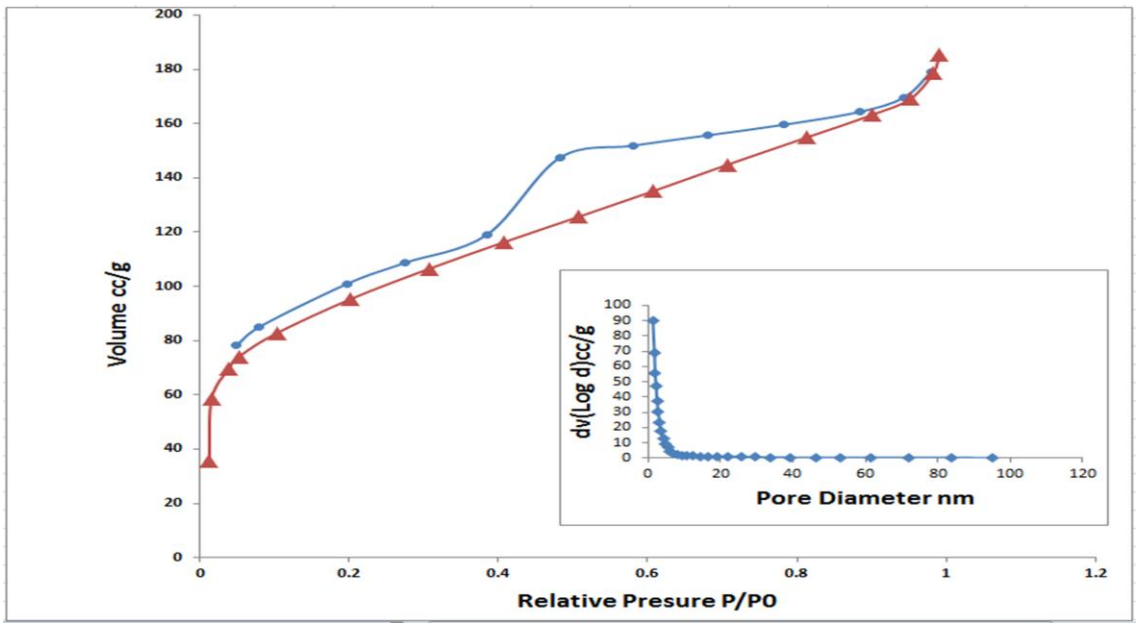

Fig.3-14: Nitrogen adsorption –desorption isotherms of RHATU-SO_4H.

Table 3-3: The result of BET analysis for RHACI and RHATUSO_4H

Sample	Specific surface area (m^2/g)	Average pore volume cm^3/g	Average pore diameter(nm)
RHACI	410	0.397	3.86
RHATU-SO_4H	357.18	0.2862	3.2051

3.3.6 Scanning electron microscope SEM

The SEM of the RHATU-SO_4H is shown in Fig. 3-15 (a and b). It seems that the surface of RHATU-SO_4H resembles to some rocky particle, which is a shell shaped randomly distributed onto surface.

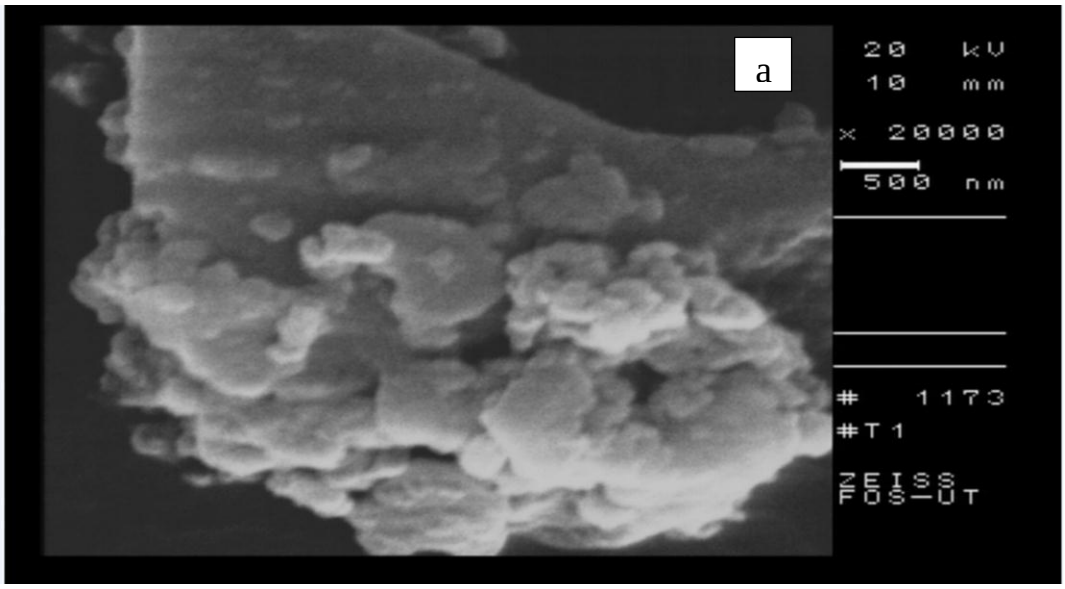

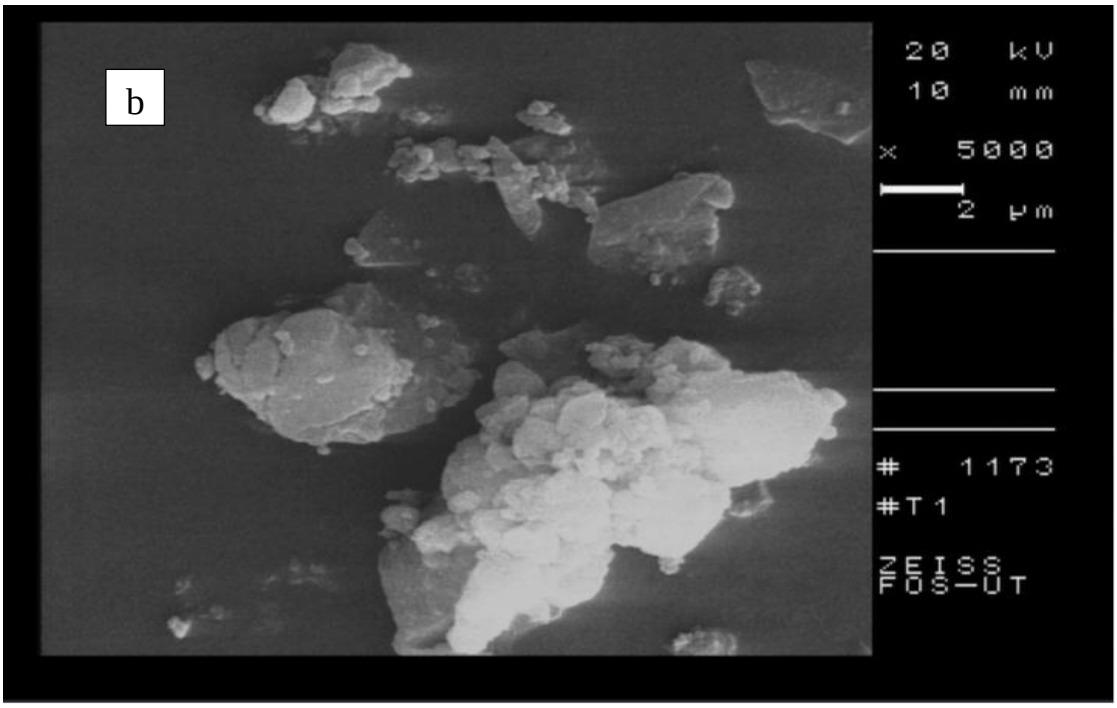

Fig3-15: SEM micrograph of RHATU-SO_4H catalyst (a) 500nm (b) 2µm.

3.3.7 Thermogravimetric analysis (TGA/DTG)

The thermogravimetric analysis (TGA) also provides some information about the organic grafting on the silica. Figure 3-16, shows the corresponding loss of mass with increase in temperature. The TGA of RHATU-SO_4H showed three distinguishing decomposition stages: First starting at (25-125)°C, attributed to lose (ca. 1.656%), and the second loss of mass (ca. 24.4%) between 225—450°C, as- attributed to the loss of the propylthiourea groups anchored onto the silica surface. The continuous weight loss (ca. 14.15%) between (450-590) °C, could be due to loss of the remaining organic propylthiourea groups associated on the silica surface and also decomposition due to condensation of silanol groups [51]. This clearly indicates that RHACCl and thiourea had been chemically grafted onto the silica surface.

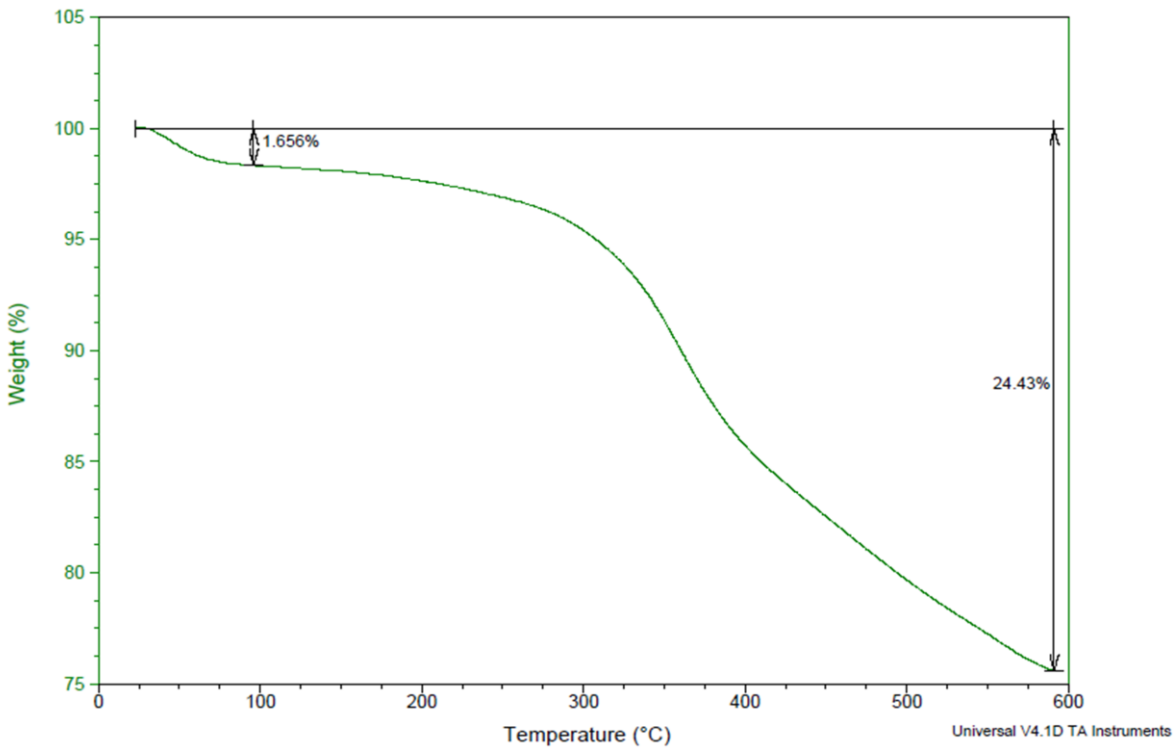

Fig.3-16: Thermal analysis (TGA) for RHATU-SO_4H catalyst

The DTG analysis for RHATU-SO_4H is shown in Fig. 3-17. The thermal degradation of RHATU-SO_4H has two main decomposition stages. The first loss of weight (ca. 1.65%) accorded about (25.87-115)°C that have maximum temperature at 40.15°C assigned to decomposition of water that adsorbed into silica surface. Second stage weight loss (ca. 24.28%) around (298.6-460)°C have maximum temperature at 355°C was attributed to decomposition of alkylthiourea [129].

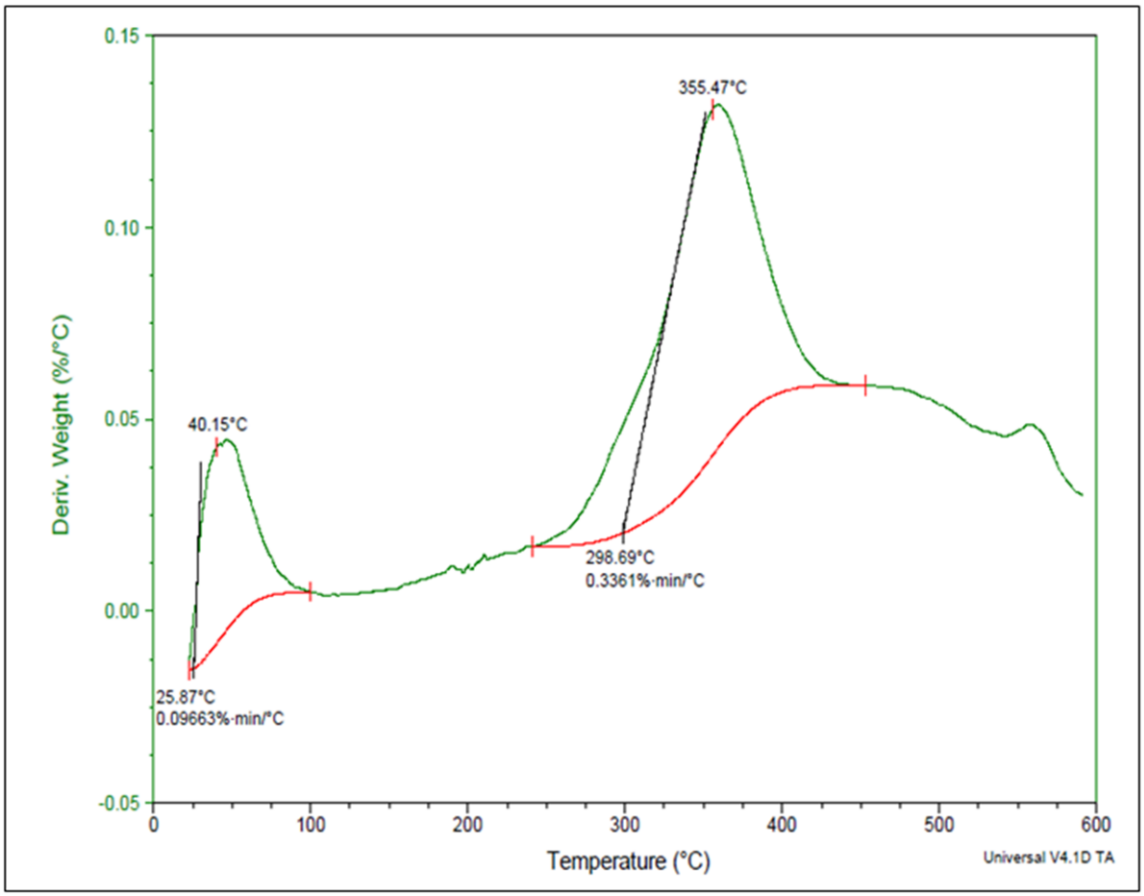

Fig. 3-17: Thermal analysis (DTG) of RHATU-SO_4H catalyst.

3.4 Surface acidity

A general perception is that the acidity of surface can be connected with activity of the catalyst. Further spectra and thermal chemical approaches are used to properties the solid surface of the catalyst [130]. In the water it can be determined the concentration of acid site on the RHATU-SO_4H. The increase Na^+ (from NaCl) with acid proton followed titrating through the standard NaOH solution with H^+. Cation exchange capacity (CEC) was obtained 15mmol/100gm of RHATU-SO_4H catalyst.

CHAPTER FOUR

4.1 Hydrolysis of cellulose over RHATU-SO_4H

The action of heterogeneous catalyst RHATU-SO_4H in addition to homogeneous thiourea for cellulose hydrolysis to glucose was studied in scheme 4-1.

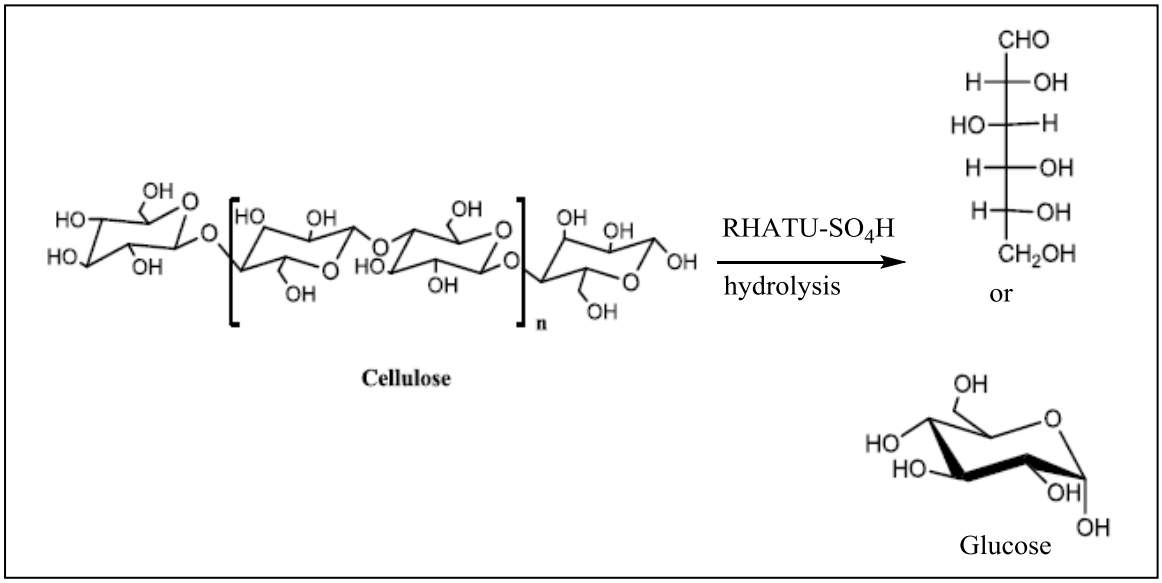

Scheme 4-1: The hydrolysis of cellulose to glucose over RHATU-SO_4H catalyst.

The hydrolysis parameters such as catalyst mass, hydrolysis time, the mass of catalyst, temperature hydrolysis, solvent impact and reusability of the catalyst were examined to improve hydrolysis conditions. The reaction mechanism over the new heterogeneous catalyst was proposed. A accompanying segments are demonstrated the action of the catalyst in details.

4.2 Catalyst study over RHATU-SO_4H

4.3 Influence of hydrolysis time

The impact of the time on the hydrolysis of cellulose over RHATU-SO_4H and homogenous thiourea are appeared in Fig.4 -1 the hydrolysis was done with 200mg of catalyst at 140°C. The first hydrolysis of cellulose during the sixth hour was 16% and it increased to a most extreme of 81% in 16h. However, it was observed that when the time increased, more than 16h, there was no change on the hydrolysis of cellulose. Therefore, best time of the cellulose hydrolysis over RHATU-SO_4H is 16h. The hydrolysis of cellulose over thiourea as a homogeneous was observed to be 27.4% at 16h. The activity of the thiourea comparing with RHATU-SO_4H was less because of the presence of amine group as homogenous active sites that have more basic. In a previous study, it is observed that the hydrolysis of cellulose over the RHA was discovered 20% in 14h and the hydrolysis of cellulose without catalyst was found to be under 20% in14h [13].

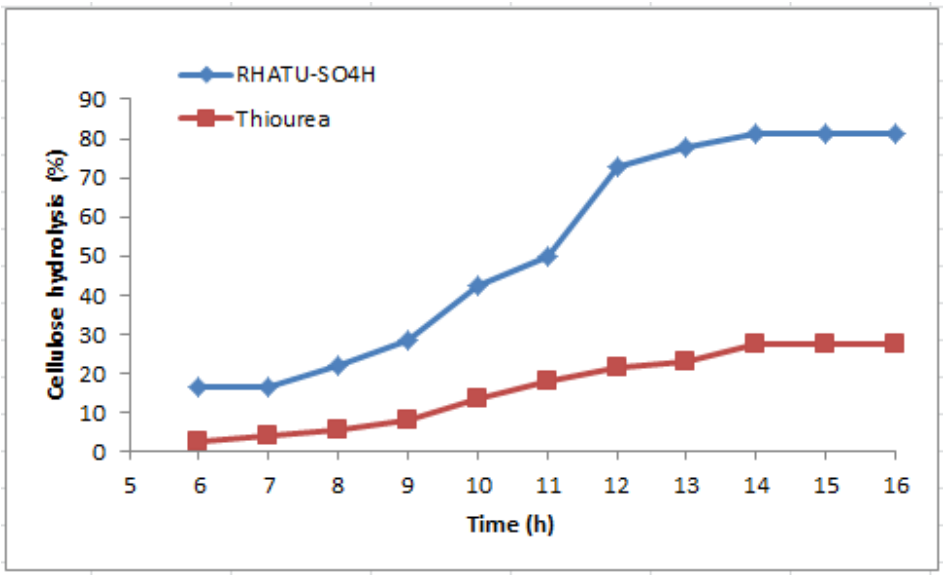

Fig.4-1: The cellulose hydrolysis to glucose over RHATU-SO4H heterogeneous catalyst and thiourea as homogenous catalyst as a function of hydrolysis time.

4.4 Influence mass of catalyst

In order to find the best catalyst mass that required to hydrolysis of cellulose, the analysis was carried out by changing the amount of RHATU-SO_4H from (150-250mg) at fixed hydrolysis temperature at 140°C, time of hydrolysis for 16h and solvent DMF/LiCl. The results have been shown in Figure 4-2 it is clearly indicated in the figure that as the mass of catalyst increased from 150 to 200 mg, the hydrolysis of cellulose into glucose raised from 68% to 81%. The increased change with the mass of catalyst could be credited to the availability of a large number of catalytically active sites destinations. However, no significant influence on cellulose hydrolysis was noticed upon increasing the mass of catalyst. It was found that 200 mg chosen as the optimum value of the RHATU-SO_4H catalyst.

.

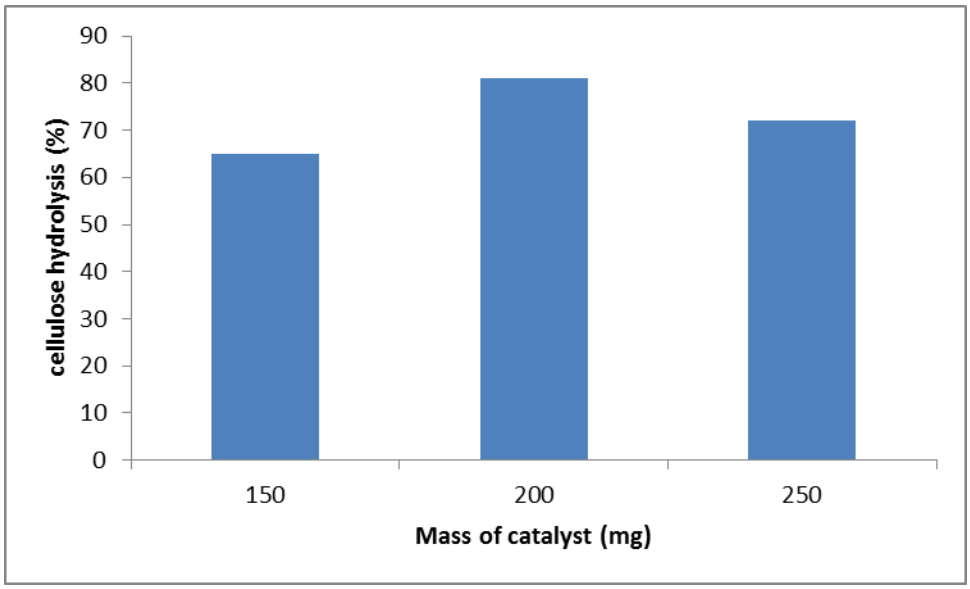

Fig.4-2:The relationship between the hydrolysis percentages of cellulose versus the used amounts of catalyst.

4.5 Influence of hydrolysis temperature

The influence of the reaction temperature on the cellulose hydrolysis over the RHATU-SO_4H is shown in Fig. 4-3, the percentage of hydrolysis increased when the temperature increased from 120 to 140 °C. The cellulose hydrolysis was ca. 81% at 140°C for 16h. which is clearly indicated that temperature greatly affects the cellulose hydrolysis .A higher temperature of hydrolysis can get higher glucose yield. Consider the way of the RHATU-SO_4H catalyst utilized (heterogeneous catalyst) in this study. This clearly demonstrates that the using of RHATU-SO_4H is successful to advance the hydrolysis of cellulose.

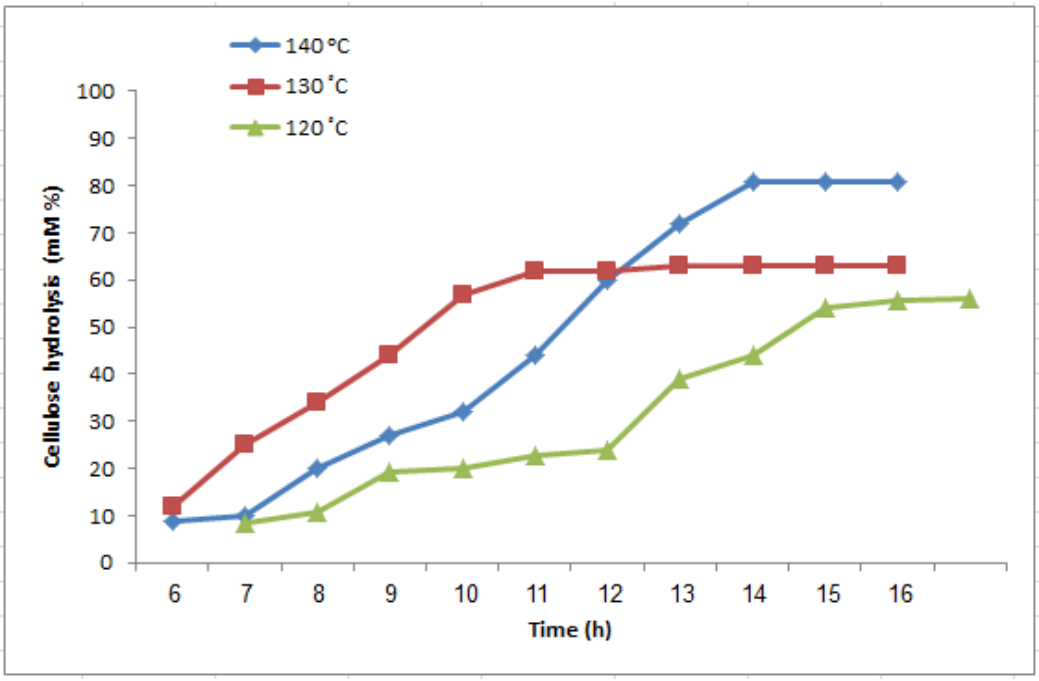

Fig.4-3: The conversion of cellulose to glucose over RHATU-SO_4H, at different temperature.

4.6 Influence of solvent effect

The solvent effect that was used as a media on the hydrolysis of cellulose over RHATU-SO_4H is represented in Table 4-1. The hydrolysis was studded over various solvents i.e. 2-mthylpropan-2-ol, Toluene and N,N-dimthylformamide (DMF). It is noted that the hydrolysis of cellulose over distinctive solvent was taken after the streaming request.

DMF>2-Methylpropan-2-ol> Toluene

The cellulose hydrolysis was relying upon the dissolvability of cellulose in the solvent. It was noticed that the cellulose was totally solvent in the DMF containing LiCl [131]. In our work it is found that the cellulose was exceptionally dissolvable in the DMF and 2-Methylpropan-2-ol containing LiCl. Most disintegration framework could shape a hydrogen bonding between layers of cellulose chain and solvent. The DMF contain more than one position ready to compose a hydrogen bonding with the cellulose and this could lead for increasing the solubility of cellulose.

Table 4-1: the cellulose hydrolysis to glucose over RHATU-SO_4H catalyst used the different solvents. The hydrolysis condition as follow: catalyst 200mg, 140°C and 16h.

Solvent	**Cellulose hydrolysis %**
DMF	81.0
2-Methylpropan-2-ol	55.8
Toluene	44.4

4.7 Catalyst recycles experiments

The main advantage of utilization of heterogeneous catalyst is ability to be reused many times. The stability of the catalyst and the activity of its active site are the main parameters of its reuse. Since the RHATU-SO_4H is heterogeneous catalyst, hence it was successfully utilized for recycling. After the first hydrolysis, it was run using the catalyst with mixture, it was then washed with hot DMF at 80°C and LiCl (this step was repeated three times) and the catalyst heated up to 100°C for 24h. Next, fresh cellulose and DMF with LiCl were added to the catalyst and washed and second runs was connected, as was a third,using the same procedure. As observed in Fig. 4-4, the yield in the second and third runs were very closly that in the first runs. These products indicated that catalytic performance doesn't lose its activity during the counts of the catalytic runs.

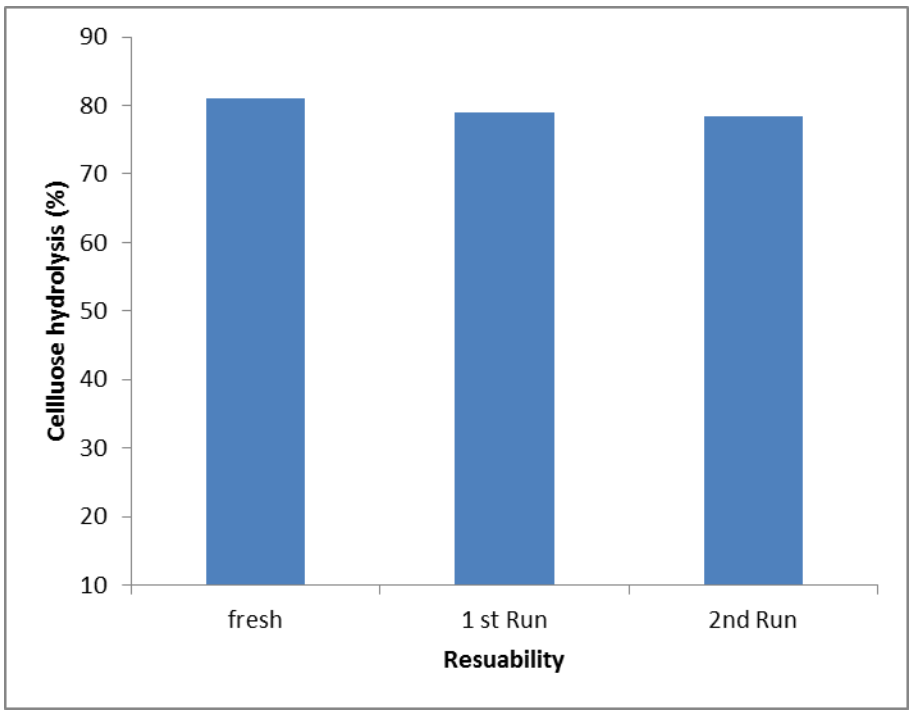

Fig. 4-4: The reusability of RHATU-SO_4H on the hydrolysis of cellulose

4.8 The efficiency of the synthesis of catalyst

The efficiency of the synthesis catalyst RHATU-SO_4H in cellulose hydrolysis that evaluated from pure cellulose, writing paper and sunflower is elucidated in Fig. 4-5. The run was done under the ideal states of the catalysis which were 200mg catalyst mass, 140 °C as the response temperature and 16h time of hydrolysis. It was watched that the pure cellulose hydrolysis was 81% while the extricated cellulose from paper and sunflower were 54%and 43.2% respectively. Obviously, it shows that the catalyst was active against cellulose hydrolysis fore pure cellulose and less active for paper and sunflower sources. It was found extracted cellulose from pure cellulose higher percentage of glucose 81% as compared with hydrolysis of cellulose from paper and sunflower that found less percentage of glucose 54% and 43.2% respectively may due to impurity of cellulose.

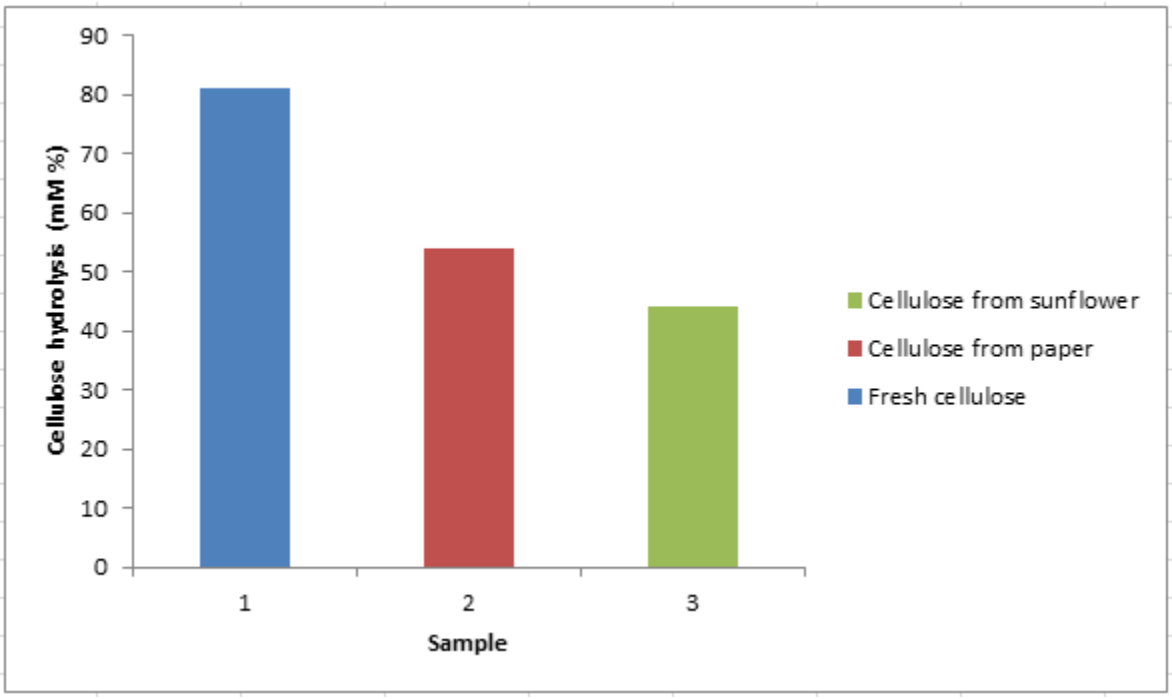

Fig. 4-5: The hydrolysis of cellulose to glucose over RHATU-SO_4H from various sources. The hydrolysis conditions were 200 mg of catalyst, 140°C hydrolysis temperature and 16h time of hydrolysis.

4.10 Conclusion

Synthesis RHACCl from rice husk ash(RHA) then replaced iodo atom from NaI with chloro atom from RHACCl to preparation new compound RHACI. The FT-IR showed the present of –C-I adsorption band at expected range. BET measurements of RHACI showed that surface area is 410 $m^2 .g^{-1}$. The XPS shown the present of iodo atom in the structure of RHACI good evidence to successfully replace iodo atom with chloro atom. Thiouera (TU) was successfully incorporated onto the RHACI via nucleophile substitution reaction to synthesis RHATU-SO_4H. The FT-IR clearly showed the presence of secondery –NH, O=S=O and C-N absorption band at expected range. The TGA shows that the catalyst is stable. BET measurements of catalyst showed that the surface area is 357 $m^2 .g^{-1}$. The elemental analysis (CHNS) of RHATU-SO_4H shows sulfur and nitrogen included into the catalyst structure. The RHATU-SO_4H was efficient for cellulose hydrolysis, with a maximum yield of glucose 81% at 140°C for 16 h. It was found that the cellulose solubility was a very important factor to make the hydrolysis much greater easily. The low hydrolysis of cellulose over thiourea comparing with cellulose hydrolysis over RHATU-SO_4H indicated that the activity of RHATU-SO_4H is a proportional to increase with acidity center.

4.12 Future prospects

In order to contiue in this field of work, the researcher would like to recommend future works.

1- Extraction of the silica from variety types of rice husks.

2- Synthesis new type of catalyst by grafting of silica with different organic compounds and use it to catalyze the hydrolysis reaction or synthesis especially those with slow rate.

3- Preparation a new hybrid organic-silica compounds which are suitable for industry field.

4- Using this catalyst to follow up to cellulose hydrolysis by working on the produced glucose and converting into alcohols as biofuel.

5- Investigation of other organic ligands and complexes to be anchored with RHACI.

6- Finding other application to extract RHA from rice husk instead of burning as waste.

References

1. Knözinger, H. and Kochloefl, K., **(2003)**. Heterogeneous catalysis and solid catalysts. Ullmann's Encyclopedia of Industrial Chemistry.
2. King, D.A. ed., **(2012)**. The chemical physics of solid surfaces and heterogeneous catalysis (Vol. 5). Elsevier science publishers B.V. Amsterdam- Oxford- New york Tokyo.
3. Guldhe, A., Moura, C.V., Singh, P., Rawat, I., Moura, E.M., Sharma, Y. and Bux, F., **(2017)**. Conversion of microalgal lipids to biodiesel using chromium-aluminum mixed oxide as a heterogeneous solid acid catalyst. Renewable Energy, 105, pp.175-182.
4. Adam, F. and Ahmed, A.E., **(2008)**. The benzylation of xylenes using heterogeneous catalysts from rice husk ash silica modified with gallium, indium and iron. Chemical Engineering Journal, 145(2), pp.328-334.
5. Andreola, F., Martín, M.I., Ferrari, A.M., Lancellotti, I., Bondioli, F., Rincón, J.M., Romero, M. and Barbieri, L., **(2013)**. Technological properties of glass-ceramic tiles obtained using rice husk ash as silica precursor. Ceramics International, 39(5), pp.5427-5435.
6. Balapour, M., Ramezanianpour, A. and Hajibandeh, E., **(2017)**. An investigation on mechanical and durability properties of mortars containing nano and micro RHA. Construction and Building Materials, 132, pp.470-477.
7. Eliche-Quesada, D., Felipe-Sesé, M.A., López-Pérez, J.A. and Infantes-Molina, A., **(2017)**. Characterization and evaluation of rice husk ash and wood ash in sustainable clay matrix bricks. Ceramics International, 43(1), pp.463-475.

8. Adam, F., Balakrishnan, S. and Wong, P.L., **(2006)**. Rice husk ash silica as a support material for ruthenium based heterogenous catalyst. Journal of Physical Science, 17(2), pp.1-13.
9. Safiuddin, M., West, J.S. and Soudki, K.A., **(2010)**. Hardened properties of self-consolidating high performance concrete including rice husk ash. Cement and Concrete Composites, 32(9), pp.708-717.
10. Javier, A.R.A., Lopez, N.E. and Juanzon, J.B.P., **(2017)**. Compressive Strength and Chloride Penetration Tests of Modified Type IP Cement with concrete Rice Ash. Procedia Engineering, 171, pp.543-548.
11. Rashid, M.H., **(2016)**. Strength Behavior of Cement Mortar Assimilating Rice Husk Ash. International Journal of Advances Agricultural Environmental Engineering., 3(2), pp.288-293.
12. Haq, I.U., Akhtar, K. and Malik, A., **(2014)**. Effect of experimental variables on the extraction of silica from the rice husk ash. Journal of Chemistry Society Pak, 36(3), p.382.
13. Mosa J. M., **(2014)**. Synthesis and Identification of Heterogeneous Catalyst from Rice Husk as Schiff Base and It's Application on the Hydrolysis of Cellulose to Glucose. M.Sc. thesis. University of Karbala. Iraq.
14. Adam, F.V., Ikotun, B.D., Patrick, D.O. and Mulaba-Bafubiandi, A.F., **(2014)**. Characterization of rice hull ash and its performance in turbidity removal from water. Particulate Science and Technology, 32(4), pp.329-333.
15. Sharma, N.K., Williams, W.S. and Zangvil, A., **(1984)**. Formation and structure of silicon carbide whiskers from rice hulls. Journal of the American Ceramic Society, 67(11), pp.715-720.

16. Lev, O., Tsionsky, M., Rabinovich, L., Glezer, V., Sampath, S., Pankratov, I. and Gun, J., **(1995)**. Organically modified sol-gel sensors. Analytical Chemistry, 67(1), pp.22A-30A.
17. Pope, E.J.A. and Mackenzie, J.D., **(1986)**. Sol-gel processing of silica: II. The role of the catalyst. Journal of Non-Crystalline Solids, 87(1-2), pp.185-198.
18. Corriu, R.J. and Leclercq, D., **(1996)**. Recent developments of molecular chemistry for sol–gel processes. Angewandte Chemie International Edition in English, 35(13-14), pp.1420-1436.
19. Singh, L.P., Bhattacharyya, S.K., Kumar, R., Mishra, G., Sharma, U., Singh, G. and Ahalawat, S., **(2014)**. Sol-Gel processing of silica nanoparticles and their applications. Advances in colloid and interface science, 214, pp.17-37.
20. Klabunde, K.J., Stark, J., Koper, O., Mohs, C., Park, D.G., Decker, S., Jiang, Y., Lagadic, I. and Zhang, D., **(1996)**. Nanocrystals as stoichiometric reagents with unique surface chemistry. The Journal of Physical Chemistry, 100(30), pp.12142-12153.
21. Hench, L.L. and West, J.K., **(1990)**. The sol-gel process. Chemical reviews, 90(1), pp.33-72.
22. Stöber, W., Fink, A. and Bohn, E., **(1968)**. Controlled growth of monodisperse silica spheres in the micron size range. Journal of colloid and interface science, 26(1), pp.62-69.
23. Matsoukas, T. and Gulari, E., **(1988)**. Dynamics of growth of silica particles from ammonia-catalyzed hydrolysis of tetra-ethyl-orthosilicate. Journal of colloid and interface science, 124(1), pp.252-261.
24. Hayder H. M. **(2012)**. Synthesis and Characterization of Heterogeneous Catalyst via Silica obtained from Iraqi Rice Husks, Ph.D. Thesis, University of Baghdad. Iraq.

25. Bettermann, P. and Liebau, F., **(1975)**. The transformation of amorphous silica to crystalline silica under hydrothermal conditions. Contributions to Mineralogy and Petrology, 53(1), pp.25-36.
26. Fournier, R.O. and Rowe, J.J., **(1966)**. Estimation of underground temperatures from the silica content of water from hot springs and wet-steam wells. American Journal of Science, 264(9), pp.685-697.
27. Suemura, N., Yoshitake, K. and Takeyama, T., Nissan Chemical Industries, Ltd., **(2016)**. Colloidal silica particles, process for producing the same, and organic solvent-dispersed silica sol, polymerizable compound-dispersed silica sol, and dicarboxylic anhydride-dispersed silica sol each obtained from the same. U.S. Patent 9,527,749.
28. Nayak, J. and Bera, J., **(2017)**. A simple method for production of humidity indicating silica gel from rice husk ash. Journal of Metals, Materials and Minerals, 19(2), pp.15-19.
29. Echeverría, J.C., Calleja, I., Moriones, P. and Garrido, J.J., **(2017)**. Fiber optic sensors based on hybrid phenyl-silica xerogel films to detect n-hexane: determination of the isosteric enthalpy of adsorption. Beilstein Journal of Nanotechnology, 8, p.475.
30. Martinez, R.G., Goiti, E., Reichenauer, G., Zhao, S., Koebel, M. and Barrio, A., **(2016)**. Thermal assessment of ambient pressure dried silica aerogel composite boards at laboratory and field scale. Energy and Buildings, 128, pp.111-118.
31. Boonbumrung, A., Sae-oui, P. and Sirisinha, C., **(2016)**. Reinforcement of multiwalled carbon nanotube in nitrile rubber: in comparison with carbon black, conductive carbon black, and precipitated silica. Journal of Nanomaterials, 2016, p.41.

32. Fruijtier-Pölloth, C., **(2012)**. The toxicological mode of action and the safety of synthetic amorphous silica—A nanostructured material. Toxicology, 294(2), pp.61-79.
33. Bogush, G.H., Tracy, M.A. and Zukoski, C.F., **(1988)**. Preparation of monodisperse silica particles: control of size and mass fraction. Journal of non-crystalline solids, 104(1), pp.95-106.
34. Babu, T.R. and Neeraja, D., **(2016)**. Rice Husk Ash as Supplementary Material in Concrete–A Review. International Journal of Chem.Tech Research, 9(5), pp.332-337.
35. Abbas, S.H., **(2015)**. Preparation And Immobilization Of Palladium (ii) And Nickel (ii) Salen Complexes Onto Mcm-41 From Rice Husk For Suzuki-Miyaura And Oxidation Reactions (Ph.D. Thesis, University Sains Malaysia).
36. Zhuravlev, L.T., **(2000)**. The surface chemistry of amorphous silica. Zhuravlev model. Colloids and Surfaces A: Physicochemical and Engineering Aspects, 173(1), pp.1-38.
37. Airoldi, C. and Arakaki, L.N., **(2001)**. Immobilization of ethylenesulfide on silica surface through sol–gel process and some thermodynamic data of divalent cation interactions. Polyhedron, 20(9), pp.929-936.
38. Dash, S., Mishra, S., Patel, S. and Mishra, B.K., **(2008)**. Organically modified silica: synthesis and applications due to its surface interaction with organic molecules. Advances in colloid and interface science, 140(2), pp.77-94.
39. Wilson, K., Lee, A.F., Macquarrie, D.J. and Clark, J.H., **(2002)**. Structure and reactivity of sol–gel sulphonic acid silicas. Applied Catalysis A: General, 228(1), pp.127-133.

40. Feher, F.J., Newman, D.A. and Walzer, J.F., **(1989)**. Silsesquioxanes as models for silica surfaces. Journal of the American Chemical Society, 111(5), pp.1741-1748.

41. Stine, J.J., **(2010)**. Analytical applications of surface-modified fused silica capillaries. Ph.D. Thesis, university of Montano Missoula, MT.

42. Paul, H., Basu, S., Bhaduri, S. and Lahiri, G.K., **(2004)**. Platinum carbonyl derived catalysts on inorganic and organic supports: a comparative study. Journal of organometallic chemistry, 689(2), pp.309-316.

43. Sahoo, S., Kumar, P., Lefebvre, F. and Halligudi, S.B., **(2007)**. Immobilized chiral diamino Ru complex as catalyst for chemo-and enantioselective hydrogenation. Journal of Molecular Catalysis A: Chemical, 273(1), pp.102-108.

44. Bae, S.J., Kim, S.W., Hyeon, T. and Kim, B.M., **(2000)**. New chiral heterogeneous catalysts based on mesoporous silica: asymmetric diethylzinc addition to benzaldehyde. Chemical Communications, (1), pp.31-32.

45. Takei, T., Houshito, O., Yonesaki, Y., Kumada, N. and Kinomura, N., **(2007)**. Porous properties of silylated mesoporous silica and its hydrogen adsorption. Journal of Solid State Chemistry, 180(4), pp.1180-1187.

46. Wang, J., Huang, L., Xue, M., Liu, L., Wang, Y., Gao, L., Zhu, J. and Zou, Z., **(2008)**. Developing a novel fluorescence chemosensor by self-assembly of Bis-Schiff base within the channel of mesoporous SBA-15 for sensitive detecting of Hg^{2+} ions. Applied Surface Science, 254(17), pp.5329-5335.

47. Hoegaerts, D., Sels, B.F., De Vos, D.E., Verpoort, F. and Jacobs, P.A., **(2000)**. Heterogeneous tungsten-based catalysts for the epoxidation of bulky olefins. Catalysis today, 60(3), pp.209-218.

48. Shi, X.Y. and Wei, J.F., **(2008)**. Selective oxidation of sulfide catalyzed by peroxotungstate immobilized on ionic liquid-modified silica with aqueous hydrogen peroxide. Journal of Molecular Catalysis A: Chemical, 280(1), pp.142-147.
49. Soundiressane, T., Selvakumar, S., Ménage, S., Hamelin, O., Fontecave, M. and Singh, A.P., **(2007)**. Ru-and Fe-based N, N′-bis (2-pyridylmethyl)-N-methyl-(1S,2S)-1,2-cyclohexanediamine complexes immobilised on mesoporous MCM-41: synthesis, characterization and catalytic applications. Journal of Molecular Catalysis A: Chemical, 270(1), pp.132-143.
50. Adam, F., Hello, K.M. and Osman, H., **(2010)**. Synthesis of Mesoporous Silica Immobilized with 3-[(Mercapto or amino) propyl] trialkoxysilane by a Simple One-pot Reaction. Chinese Journal of Chemistry, 28(12), pp.2383-2388.
51. Adam, F., Hello, K.M. and Osman, H., **(2010)**. The heterogenation of melamine and its catalytic activity. Applied Catalysis A: General, 382(1), pp.115-121.
52. Hello, K.M., Mohammad, A.T. and Sager, A.G., **(2016)**. Solid Urea Sulfate Catalyst for Hydrolysis of Cellulose. Waste and Biomass Valorization, pp.1-10.
53. Adam, F., Chew, T.S., Mannyarasai, H., Appaturi, J.N. and Hello, K.M., **(2013)**. Synthesis and characterization of silica–imidazole mesostructured composite from agricultural biomass. Microporous and Mesoporous Materials, 167, pp.245-248.
54. Adam, F., Hassan, H.E. and Hello, K.M., **(2012)**. The synthesis of N-heterocyclic carbene–silica nano-particles and its catalytic activity in the cyclization of glycerol. Journal of the Taiwan Institute of Chemical Engineers, 43(4), pp.619-630.

55. Hello, K.M., **(2010)**. The heterogenation of saccharine, melamine and sulfonic acid onto rice husk ash silica and their catalytic activity in esterification reaction. Ph.D. Thesis, University of sains Malaysia, Malaysia.
56. Adam, F., Hello, K.M. and Chai, S.J., **(2012)**. The heterogenization of l-phenylalanine–Ru (III) complex and its application as catalyst in esterification of ethyl alcohol with acetic acid. Chemical Engineering Research and Design, 90(5), pp.633-642.
57. Örgül, S. and Atalay, Ü., **(2002)**. Reaction chemistry of gold leaching in thiourea solution for a Turkish gold ore. Hydrometallurgy, 67(1), pp.71-77.
58. Roberts, J.M., Fini, B.M., Sarjeant, A.A., Farha, O.K., Hupp, J.T. and Scheidt, K.A., **(2012)**. Urea metal–organic frameworks as effective and size-selective hydrogen-bond catalysts. Journal of the American Chemical Society, 134(7), pp.3334-3337.
59. Luan, Y., Zheng, N., Qi, Y., Tang, J. and Wang, G., **(2014)**. Merging metal–organic framework catalysis with organocatalysis: A thiourea functionalized heterogeneous catalyst at the nanoscale. Catalysis Science & Technology, 4(4), pp.925-929.
60. Dove, A.P., Pratt, R.C., Lohmeijer, B.G., Waymouth, R.M. and Hedrick, J.L., **(2005)**. Thiourea-based bifunctional organocatalysis: supramolecular recognition for living polymerization. Journal of the American Chemical Society, 127(40), pp.13798-13799.
61. Lehnherr, D., Ford, D.D., Bendelsmith, A.J., Kennedy, C.R. and Jacobsen, E.N., **(2016)**. Conformational control of chiral amido-thiourea catalysts enables improved activity and enantioselectivity. Organic Letters, 18(13), pp.3214-3217.

62. Yue, Y., **(2015)**. Cellulose Nanofibers from Energycane Bagasse and Their Applications in Core-Shell Structured Hydrogels. Ph.D. Thesis, Louisiana State University and Agricultural and Mechanical College.
63. Nishino, T., Matsuda, I. and Hirao, K., **(2004)**. All-cellulose composite. Macromolecules, 37(20), pp.7683-7687.
64. Hello, K.M., Mihsen, H.H., Mosa, M.J. and Magtoof, M.S., **(2015)**. Hydrolysis of cellulose over silica-salicylaldehyde phenylhydrazone catalyst. Journal of the Taiwan Institute of Chemical Engineers, 46, pp.74-81.
65. Moon, R.J., Martini, A., Nairn, J., Simonsen, J. and Youngblood, J., **(2011)**. Cellulose nanomaterials review: structure, properties and nanocomposites. Chemical Society Reviews, 40(7), pp.3941-3994.
66. Dhepe, P.L. and Fukuoka, A., **(2007)**. Cracking of cellulose over supported metal catalysts. Catalysis Surveys from Asia, 11(4), pp.186-191.
67. Bergenstråhle, M., Matthews, J., Crowley, M. and Brady, J., **(2010)**. Cellulose crystal structure and force fields. In International Conference on Nanotechnology for the forest products industry. Otaniemi, Espoo, Finland.
68. Röhrling, J., Potthast, A., Rosenau, T., Lange, T., Ebner, G., Sixta, H. and Kosma, P., **(2002)**. A novel method for the determination of carbonyl groups in cellulosics by fluorescence labeling. 1. Method development. Biomacromolecules, 3(5), pp.959-968.
69. Huang, Y.B. and Fu, Y., **(2013)**. Hydrolysis of cellulose to glucose by solid acid catalysts. Green Chemistry, 15(5), pp.1095-1111.
70. Lai, D.M., Deng, L., Li, J., Liao, B., Guo, Q.X. and Fu, Y., **(2011)**. Hydrolysis of cellulose into glucose by magnetic solid acid. ChemSusChem, 4(1), pp.55-58.

71. Li, C. and Zhao, Z.K., **(2007)**. Efficient Acid-Catalyzed Hydrolysis of Cellulose in Ionic Liquid. Advanced Synthesis & Catalysis, 349(11-12), pp.1847-1850.

72. Vasconcelos, N.F., Feitosa, J.P.A., da Gama, F.M.P., Morais, J.P.S., Andrade, F.K., de Souza, M.D.S.M. and de Freitas Rosa, M., **(2017)**. Bacterial cellulose nanocrystals produced under different hydrolysis conditions: Properties and morphological features. Carbohydrate Polymers, 155, pp.425-431.

73. Onda, A., Ochi, T. and Yanagisawa, K., **(2008)**. Selective hydrolysis of cellulose into glucose over solid acid catalysts. Green Chemistry, 10(10), pp.1033-1037.

74. Sulman, E.M., Matveeva, V.G., Manaenkov, O.V., Filatova, A.E., Kislitza, O.V., Doluda, V.Y., Rebrov, E.V., Sidorov, A.I. and Shimanskaya, E.I., **(2016)**. November. Cellulose hydrogenolysis with the use of the catalysts supported on hypercrosslinked polystyrene. In A.H. Bhat and N.B. Yahya eds., AIP Conference Proceedings (Vol. 1787, No. 1,pp. 030004). AIP Publishing.

75. Suganuma, S., Nakajima, K., Kitano, M., Yamaguchi, D., Kato, H. and Hayashi, S., **(2008)**. Hydrolysis of cellulose by amorphous carbon bearing SO3H, COOH, and OH groups. Journal of the American Chemical Society, 130(38), pp.12787-12793.

76. Wiredu, B. and Amarasekara, A.S., **(2014)**. Synthesis of a silica-immobilized Brönsted acidic ionic liquid catalyst and hydrolysis of cellulose in water under mild conditions. Catalysis Communications, 48, pp.41-44.

77. Kim, J.S., Lee, Y.Y. and Torget, R.W., **(2001)**. Cellulose hydrolysis under extremely low sulfuric acid and high-temperature conditions. Applied biochemistry and biotechnology, 91(1-9), pp.331-340.

78. Verma, D., Tiwari, R. and Sinha, A.K., **(2013)**. Depolymerization of cellulosic feedstocks using magnetically separable functionalized graphene oxide. Royal Scociety of Chemistry Advances, 3(32), pp.13265-13272.
79. Wang, H., Zhang, C., He, H. and Wang, L., **(2012)**. Glucose production from hydrolysis of cellulose over a novel silica catalyst under hydrothermal conditions. Journal of Environmental Sciences, 24(3), pp.473-478.
80. Cai, H., Li, C., Wang, A., Xu, G. and Zhang, T., **(2012)**. Zeolite-promoted hydrolysis of cellulose in ionic liquid, insight into the mutual behavior of zeolite, cellulose and ionic liquid. Applied Catalysis B: Environmental, 123, pp.333-338.
81. Amarasekara, A.S. and Wiredu, B., **(2012)**. A comparison of dilute aqueous p-toluenesulfonic and sulfuric acid pretreatments and saccharification of corn stover at moderate temperatures and pressures. Bioresource technology, 125, pp.114-118.
82. Shuai, L. and Pan, X., **(2012)**. Hydrolysis of cellulose by cellulase-mimetic solid catalyst. Energy & Environmental Science, 5(5), pp.6889-6894.
83. Chambon, F., Rataboul, F., Pinel, C., Cabiac, A., Guillon, E. and Essayem, N., **(2011)**. Cellulose hydrothermal conversion promoted by heterogeneous Brønsted and Lewis acids: remarkable efficiency of solid Lewis acids to produce lactic acid. Applied Catalysis B: Environmental, 105(1), pp.171-181.
84. Zhang, Y.H.P., Cui, J., Lynd, L.R. and Kuang, L.R., **(2006)**. A transition from cellulose swelling to cellulose dissolution by o-phosphoric acid: evidence from enzymatic hydrolysis and supramolecular structure. Biomacromolecules, 7(2), pp.644-648.

85. Fan, G., Liao, C., Fang, T., Wang, M. and Song, G., **(2013)**. Hydrolysis of cellulose catalyzed by sulfonated poly (styrene-co-divinylbenzene) in the ionic liquid 1-n-butyl-3-methylimidazolium bromide. Fuel processing technology, 116, pp.142-148.
86. Takagaki, A., Nishimura, M., Nishimura, S. and Ebitani, K., **(2011)**. Hydrolysis of sugars using magnetic silica nanoparticles with sulfonic acid groups. Chemistry Letters, 40(10), pp.1195-1197.
87. Kobayashi, H., Ohta, H. and Fukuoka, A., **(2012)**. Conversion of lignocellulose into renewable chemicals by heterogeneous catalysis. Catalysis Science & Technology, 2(5), pp.869-883.
88. Passe-Coutrin, N., Altenor, S., Cossement, D., Jean-Marius, C. and Gaspard, S., **(2008)**. Comparison of parameters calculated from the BET and Freundlich isotherms obtained by nitrogen adsorption on activated carbons: A new method for calculating the specific surface area. Microporous and Mesoporous Materials, 111(1), pp.517-522.
89. Sing, K., **(2001)**. The use of nitrogen adsorption for the characterisation of porous materials. Colloids and Surfaces A: Physicochemical and Engineering Aspects, 187, pp.3-9.
90. Nishiyama, H., Suga, M., Ogura, T., Maruyama, Y., Koizumi, M., Mio, K., Kitamura, S. and Sato, C., **(2010)**. Reprint of: Atmospheric scanning electron microscope observes cells and tissues in open medium through silicon nitride film. Journal of structural biology, 172(2), pp.191-202.
91. Zhao, C., Wang, W., Yu, Z., Zhang, H., Wang, A. and Yang, Y., **(2010)**. Nano-CaCO 3 as template for preparation of disordered large mesoporous carbon with hierarchical porosities. Journal of Materials Chemistry, 20(5), pp.976-980.
92. Basics of X-ray Diffraction. [Online]. [Accessed 15 march **2017**]. Available from World Wide Web. WWW. S cintag. Com.

93. Maslem E.N, FOXA., Okeefe M.A., **(2004)**. X-ray Scattering. (Ed), International Table for crystallography, Vol. C (kiuwer Academic, Dordrecht, pp554.

94. Feidenhans, R., **(1989)**. Surface structure determination by X-ray diffraction. Surface Science Reports, 10(3), pp.105-188.

95. Danilatos, G.D., **(1990)**. Theory of the gaseous detector device in the environmental scanning electron microscope. Advances in Electronics and Electron Physics, 78, pp.1-102.

96. Pavia, D.L., Lampman, G.M., Kriz, G.S. and Vyvyan, J.A., **(2008)**. Introduction to spectroscopy. Cengage Learning, Department of chemistry western Washington University Bellingham, Washington.

97. Griffiths, P.R. and De Haseth, J.A., **(2007)**. Fourier transforms infrared spectrometry (Vol. 171). John Wiley & Sons 2^{end} , New Jersey.

98. Guanhua, F., **(2012)**. The synthesis and characterization of phosphoric acids for the surface medication study on Indium tin oxide, M.Sc. Thesis. Gorgia Institute of Techenology, USA.

99. Markovic, G. and Visakh, P.M. eds., **(2016)**. Rubber Nano Blends: Preparation, Characterization and Applications. Springer.

100. Gupta, S.D., Mukhopadhyay, R., Baranwal, K.C. and Bhowmick, A.K., **(2013)**. Reverse Engineering of Rubber Products: Concepts, Tools, and Techniques. CRC Press, London.

101. Ahmed, A.E. and Adam, F., **(2007)**. Indium incorporated silica from rice husk and its catalytic activity. Microporous and mesoporous materials, 103(1), pp.284-295.

102. Adam, F., Osman, H., and Hello, K. M., **(2009)**. The immobilization of 3-(chloropropyl)triethoxysilane onto silica by a simple one-pot synthesis, Journal of Colloid Interface Science, 331 , 143–147.

103. Ahmed, I. and Parish, R.V., **(1993)**. Insoluble Ligands and their Applications: IV. Polysiloxane-bis (2-aminoethyl) amine Ligands and some Derivatives. Journal of organometallic chemistry, 452(1-2), pp.23-28.
104. Adam, F., Hello, K.M. and Ali, T.H., **(2011)**. Solvent free liquid-phase alkylation of phenol over solid sulfanilic acid catalyst. Applied Catalysis A: General, 399(1), pp.42-49.
105. Hello, K.M., Mihsen, H. and Mosa, M., **(2014)**. Modification of silica with 2, 4-dinitrophenylhydrazanomethylphenol for monosaccharide productions. Iranian Journal of Catalysis, 4(3), pp.195-203.
106. Aboody, M.H., **(2013)**. Extraction of Cellulose from some Industrial and Plant's Waste and its hydrolysis using new heterogeneous catalyst. Ph.D. Thesis, Basrah University.
107. Adam, F. and Iqbal, A., **(2010)**. The oxidation of styrene by chromium–silica heterogeneous catalyst prepared from rice husk. Chemical Engineering Journal, 160(2), pp.742-750.
108. Da Cruz, R.S., e Silva, J.M.D.S., Arnold, U. and Schuchardt, U., **(2001)**. Catalytic activity and stability of a chromium containing silicate in liquid phase cyclohexane oxidation. Journal of Molecular Catalysis A: Chemical, 171(1), pp.251-257.
109. López-Aranguren, P., Saurina, J., Vega, L.F. and Domingo, C., **(2012)**. Sorption of tryalkoxysilane in low-cost porous silicates using a supercritical CO_2 method. Microporous and Mesoporous Materials, 148(1), pp.15-24.
110. Yalcin, N. and Sevinc, V., **(2001)**. Studies on silica obtained from rice husk. Ceramics international, 27(2), pp.219-224.
111. Adam, F. and Batagarawa, M.S., **(2013)**. Tetramethylguanidine–silica nanoparticles as an efficient and reusable catalyst for the

synthesis of cyclic propylene carbonate from carbon dioxide and propylene oxide. Applied Catalysis A: General, 454, pp.164-171.

112. Thuadaij, N. and Nuntiya, A., **(2008)**. Synthesis and characterization of nanosilica from rice husk ash prepared by precipitation method. J. Nat. Sci. Special Issue on Nanotechnology, 7(1), pp.59-65.
113. Yalcin, N. and Sevinc, V., **(2001)**. Studies on silica obtained from rice husk. Ceramics international, 27(2), pp.219-224.
114. Beccat, P., Da Silva, P., Huiban, Y. and Kasztelan, S., **(1999)**. Quantitative surface analysis by XPS (X-ray photoelectron spectroscopy): application to hydrotreating catalysts. Oil & Gas Science and Technology, 54(4), pp.487-496.
115. Oehr, C., **(2003)**. Plasma surface modification of polymers for biomedical use. Nuclear Instruments and Methods in Physics Research Section B: Beam Interactions with Materials and Atoms, 208, pp.40-47.
116. Millard, M.M., Foy, C.D., Coradetti, C.A. and Reinsel, M.D., **(1990)**. X-ray photoelectron spectroscopy surface analysis of aluminum ion stress in barley roots. Plant physiology, 93(2), pp.578-583.
117. Yang, Q., Liu, J., Yang, J., Kapoor, M.P., Inagaki, S. and Li, C., **(2004)**. Synthesis, characterization, and catalytic activity of sulfonic acid-functionalized periodic mesoporous organosilicas. Journal of Catalysis, 228(2), pp.265-272.
118. Hanif, M.A., **(2014)**. Characterization of Pd nanoparticles and of silica-supported Pd-catalysts for the Suzuki-Miyaura reaction. Ph.D. Thesis, Queen, University Canada.
119. Su, C., Chen, C.C., Tsai, C.S., Lin, J.L. and Lin, J.C., **(2006)**. The Adsorption, Thermal Desorption and Photochemistry of Methyl

Iodide on an Ag-Covered TiO2 (110) Surface. Journal of the Chinese Chemical Society, 53(4), pp.803-813.

120. Pinto, S., Alves, P., Matos, C.M., Santos, A.C., Rodrigues, L.R., Teixeira, J.A. and Gil, M.H., **(2010)**. Poly (dimethyl siloxane) surface modification by low pressure plasma to improve its characteristics towards biomedical applications. Colloids and Surfaces B: Biointerfaces, 81(1), pp.20-26.
121. Truong, L.T., Larsen, Å., Holme, B., Diplas, S., Hansen, F.K., Roots, J. and Jørgensen, S., **(2010)**. Dispersibility of silane-functionalized alumina nanoparticles in syndiotactic polypropylene. Surface and Interface Analysis, 42(6-7), pp.1046-1049.
122. Van Stipdonk, M.J., Santiago, V., Schweikert, E.A., Chusuei, C.C. and Goodman, D.W., **(2000)**. Secondary ion emission from keV energy atomic and polyatomic projectile impacts on sodium iodate. International Journal of Mass Spectrometry, 197(1), pp.149-161.
123. Xiong, L., Sekiya, E.H., Sujaridworakun, P., Wada, S. and Saito, K., **(2017)**. Burning temperature dependence of rice husk ashes in structure and property. Journal of Metals, Materials and Minerals, 19(2).
124. Ameram, N. and Adam, F., **(2015)**. Iron Carbonyl Thiourea Hybrid Material Based on Functionalised Silica from Rice Husk Ash for Oxidation of Limonene. Procedia Chemistry, 16, pp.700-708.
125. Gopalakrishnan, S., Jungwirth, P., Tobias, D.J. and Allen, H.C., **(2005)**. Air− liquid interfaces of aqueous solutions containing ammonium and sulfate: Spectroscopic and molecular dynamics studies. The Journal of Physical Chemistry B, 109(18), pp.8861-8872.
126. Kandile, N.G., Razek, T.M., Al-Sabagh, A.M. and Khattab, M.M., **(2014)**. Synthesis and evaluation of some amine compounds having

surface active properties as H 2 S scavenger. Egyptian Journal of Petroleum, 23(3), pp.323-329.

127. Adam, F. and Chua, J.H., **(2004)**. The adsorption of palmytic acid on rice husk ash chemically modified with Al (III) ion using the sol–gel technique. Journal of colloid and interface science, 280(1), pp.55-61.
128. Thommes, M., **(2010)**. Physical adsorption characterization of nanoporous materials. Chemie Ingenieur Technik, 82(7), pp.1059-1073.
129. Liu, K., Feng, Q., Yang, Y., Zhang, G., Ou, L. and Lu, Y., **(2007)**. Preparation and characterization of amorphous silica nanowires from natural chrysotile. Journal of Non-Crystalline Solids, 353(16), pp.1534-1539.
130. Felix, S.P., Savill-Jowitt, C. and Brown, D.R., **(2005)**. Base adsorption calorimetry for characterising surface acidity: a comparison between pulse flow and conventional "static" techniques. Thermochimica acta, 433(1), pp.59-65.
131. Dutta, S., De, S., Alam, M.I., Abu-Omar, M.M. and Saha, B., **(2012)**. Direct conversion of cellulose and lignocellulosic biomass into chemicals and biofuel with metal chloride catalysts. Journal of catalysis, 288, pp.8-15.